Improved accuracy in adiabatic cross sections for low-energy rotational and vibrational excitation of molecules by electron impact

Michael A. Morrison, Mehran Abdolsalami,* and Brian K. Elza
Department of Physics and Astronomy, University of Oklahoma, Norman, Oklahoma 73019-0225
(Received 13 September 1990)

We have developed a first-order adiabatic scattering theory for the calculation of low-energy rovibrational cross sections. This theory is more efficient computationally than a full coupled-state method because it transforms coupling of intermediate states into a parametric dependence on nuclear coordinates, and it is more accurate than the conventional adiabatic nuclei method because it correctly conserves energy in the entrance and exit channels. As formulated, this theory can easily be implemented using available computer programs that solve fixed-nuclei scattering equations. We derive this theory for rotational and vibrational excitation with both local and nonlocal potentials and assess it by application to e-H_2 collisions.

I. INTRODUCTION

The problem of accurately calculating near-threshold inelastic electron-molecule cross sections has been vexatious for years. Near-threshold cross sections are important for applied research in such areas as gas-discharge devices and pollution control.[1] These cross sections also provide fundamental insight into a uniquely sensitive, purely quantum-mechanical collision process. Yet, data on near-threshold electron-molecule scattering remains fragmentary,[2] discordant with existing experimental results,[3] and subject to a variety of theoretical concerns.[4–7]

At present, two approaches to calculating low-energy electron-molecule cross sections predominate. In the most rigorous, laboratory-frame close-coupling (LFCC) theory,[8–10] the electron-molecule wave function is expanded in complete sets of rotational and vibrational eigenfunctions of the target and angular momentum eigenfunctions of the projectile. In the most widely used approach, the adiabatic-nuclei (AN) theory,[11–16] one simplifies the LFCC equations via two approximations. First, one separates target and projectile variables in the system wave function,[17] which allows independent treatment of the collision dynamics and purely kinematic effects and greatly reduces the computational effort required to solve the scattering equations. Second, one equates the energy of the projectile in the exit channel to its energy in the entrance channel. This "target-state degeneracy" approximation ignores the energy lost by the electron in exciting the target and enables one to calculate the transition matrix on the energy-momentum shell. The comparative simplicity of AN calculations have made possible studies of rotational and vibrational excitation on systems far more complicated than those to which one can apply LFCC theory.[18]

But for collisions near threshold neither approach is satisfactory. On the one hand, extensive coupling of rotational, vibrational, and angular momentum eigenfunctions by the nonspherical, nonlocal electron-molecule potential makes converging LFCC cross sections computationally impossible (to date) for systems except e-H_2. On the other, a breakdown of the assumptions of AN theory at low scattering energies[16] introduces significant errors in near-threshold cross sections,[19,20] errors that for vibrational excitation are enormous.[21] These problems are illustrated in Fig. 1, which compares LFCC and AN cross sections for pure vibrational and rovibrational excitations of H_2.

The alternative method presented in this paper produces low-energy cross sections that are significantly more accurate than those of AN theory but does so without incurring the computational demands of LFCC calculations. Figure 1 shows the rationale for our approach: if in the LFCC equations all channel energies are artificially set equal to the entrance-channel energy, then the resulting "degenerate LFCC" cross sections are nearly identical to those obtained in an AN calculation. The AN and degenerate-LFCC calculations share the approximation of target-state degeneracy, but the latter does not make the additional assumption of separation of variables. In the present method we retain the assumption of separation of variables but use the correct energies for the entrance and exit channels. Figure 1 shows that the resulting formalism, which is almost as simple computationally as the AN method, is almost as accurate as the far more CPU-intensive LFCC method.[22]

The mathematical structure of this formalism, which we call the first-order nondegenerate adiabatic (FONDA) theory,[23] differs little from that of the AN method. Both are based on the solution of fixed-nuclei (FN) scattering equations in a body-fixed (BF) reference frame, followed by transformation of an approximate scattering matrix into the (space-fixed) laboratory frame (LF) where cross sections are calculated. Consequently, the FONDA method should be easily applicable to a variety of electron-molecule systems. Moreover, its implementation requires very little code development, because most of the necessary machinery is available from sources such as the CPC Program Library.[24] The latter includes, for example, thoroughly tested programs for calculating various

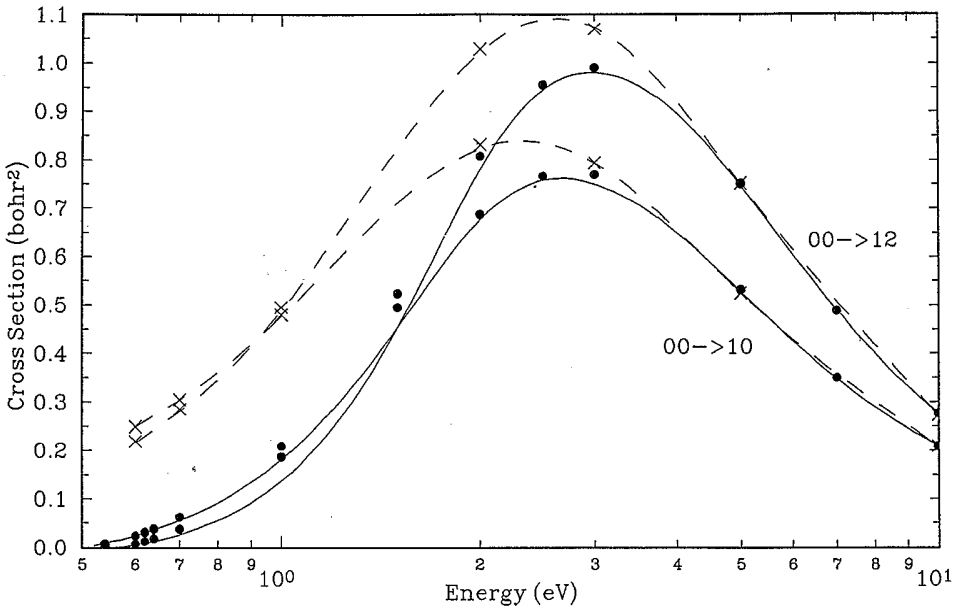

FIG. 1. The effect of various approximations to the nuclear dynamics on the accuracy of pure vibrational excitation (0,0→1,0) and rovibrational excitation (0,0→1,2) e-H_2 cross sections: rigorous treatment via the LFCC method (solid curves), "degenerate LFCC" calculations in which channel energies are artificially set equal to one another (crosses), the AN approximation (long-dashed curve), and the FONDA method (dots).

components of the interaction potential[25] and coupling matrix elements, solving differential scattering equations,[26] evaluating cross sections from scattering matrices,[27] and other tasks.

In two earlier brief papers[23,28] we introduced the FONDA approach and presented a few results for e-H_2 scattering in a local-potential approximation. Here we derive the equations of the FONDA method for rotational and vibrational excitation for local and nonlocal potentials (Sec. II). Then, following a brief summary of the necessary numerical procedures (Sec. III), we present a study of rotational and vibrational excitation of H_2 (Sec. IV). We have chosen this system for the first application of the FONDA method because it is sufficiently simple for us to calculate benchmark LFCC cross sections with which to assess the accuracy of approximate theories. Unless otherwise stated, atomic units are used throughout this paper.

II. THEORY

To clarify our derivation of the FONDA theory and to situate the method in a context of other formulations, we begin with a brief overview that does not explicitly engage the major complications of the electron-molecule system. Then, in Sec. II C, we introduce these features and derive the FONDA reactance matrix for a local potential. In Sec. II D we extend the theory to potentials that contain nonlocal terms.[29]

A. Preliminaries

Since we are interested in scattering energies well below the first electronically inelastic threshold, we first project out of the time-independent Schrödinger equation the ground $X\,^1\Sigma_g^+$ (Born-Oppenheimer) electronic wave function of the (homonuclear diatomic) target. The resulting "reduced" Schrödinger equation depends on the coordinates of the projectile ($\mathbf{r}$) and of the nuclei of the target, which are the coordinates of the internuclear axis in the LF ($\mathbf{R}$), i.e.,

$$(\hat{T}_e+\hat{\mathcal{H}}_m^{(n)}+\hat{V}-E)\psi_0(\mathbf{r},\mathbf{R})=0\ , \tag{1}$$

where $\hat{T}_e$ is the projectile's kinetic energy and E is the total energy.

An essential complicating feature of the scattering equation is that $\psi_0(\mathbf{r},\mathbf{R})$ cannot (rigorously) be separated as a product of a function of $\mathbf{r}$ and a function of $\mathbf{R}$, because the interaction potential $\hat{V}$ "couples" these variables. This potential includes[30] (i) a static term, which is the average of the bound-free Coulomb interactions over the ground-state molecular electronic function, (ii) a nonlocal exchange term which incorporates the antisymmetrization requirement, and (iii) a correlation/polarization term which approximates induced polarization and bound-free correlation effects.

The molecular dynamics are represented in Eq. (1) by the nuclear Hamiltonian, which is the sum of the rotational Hamiltonian, the vibrational Hamiltonian, the nucleus-nucleus Coulomb potential, and the ground-state electronic energy:

$$\hat{\mathcal{H}}_m^{(n)}=\hat{\mathcal{H}}_m^{(r)}+\hat{\mathcal{H}}_m^{(v)}+\hat{V}^{(n)}+\mathcal{E}_0^{(e)}(R)\ . \tag{2}$$

This Hamiltonian defines the energies of the target states via its eigenvalue equation; letting the index ν denote rotational (j,m_j) and vibrational (v) quantum numbers, we can write this equation as

$$\hat{\mathcal{H}}_m^{(n)}\chi_\nu(\mathbf{R})=\varepsilon_\nu\chi_\nu(\mathbf{R})\ . \tag{3}$$

For a diatomic molecule with rotational constant B_v and vibrational constants ω_e, x_e, and D_e, the eigenvalues are given approximately by[31,32]

$$\varepsilon_\nu=\omega_e(v+\tfrac{1}{2})-\omega_e x_e(v+\tfrac{1}{2})^2 +B_v j(j+1)-D_e j^2(j+1)^2\ . \tag{4}$$

Conservation of energy in the inelastic collision $v_0,j_0\to v,j$ requires that

$$E=\tfrac{1}{2}k_0^2+\varepsilon_0=\tfrac{1}{2}k_{vj}^2+\varepsilon_\nu\ . \tag{5}$$

The assumption of target-state degeneracy in the AN method violates this requirement, and Fig. 1 shows that this violation is primarily responsible for the breakdown of that method near threshold.

To develop the FONDA alternative, we begin with the exact integral equation for the scattering amplitude $f_{\nu\nu_0}(\hat{\mathbf{r}})$ which appears in the asymptotic (plane-wave) boundary conditions[6]

$$\psi_0(\mathbf{r},\mathbf{R})\underset{r\to\infty}{\sim}(2\pi)^{-3/2}\left[e^{-i\mathbf{k}_0\cdot\mathbf{r}}\chi_{\nu_0}(\mathbf{R}) +\sum_\nu^{(\text{open})}\frac{e^{ik_{vj}r}}{r}f_{\nu\nu_0}(\hat{\mathbf{r}})\chi_\nu(\mathbf{R})\right]\ . \tag{6}$$

For an electron which induces the excitation $\nu_0\to\nu$ and scatters in the direction $\mathbf{k}_{vj}=k_{vj}\hat{\mathbf{r}}$, the (post) form of this equation is[33]

$$f_{\nu\nu_0}(\hat{\mathbf{r}})=-(2\pi)^{1/2}\int e^{-i\mathbf{k}_{vj}\cdot\mathbf{r}'}\chi_\nu^*(\mathbf{R})\hat{V}(\mathbf{r}',\mathbf{R})\psi_0(\mathbf{r}',\mathbf{R})d\mathbf{r}'d\mathbf{R}\ . \tag{7}$$

Note that in (7) the exit-channel corresponds (properly) to a product of wave functions for the final target state ν and for an outgoing plane wave of energy $k_{vj}^2/2$. Just as the FONDA theory preserves energy conservation (5), so does it preserve this correspondence.

To solve (7) exactly one could expand ψ_0 in the complete set of target states $\{\chi_\nu(\mathbf{R})\}$. In terms of channel scattering functions $\zeta_{\nu\nu_0}(\mathbf{r}')$, the resulting coupled integral equation, which we shall need in Sec. II B, is

$$f_{\nu\nu_0}(\hat{\mathbf{r}})=-(2\pi)^{1/2}\int e^{-i\mathbf{k}_{vj}\cdot\mathbf{r}'}\sum_{\nu'}V_{\nu\nu'}(\mathbf{r}')\zeta_{\nu'\nu_0}(\mathbf{r}')d\mathbf{r}'\ . \tag{8}$$

Nonseparability of the electron-molecule scattering function ψ_0 appears as coupling of intermediate target states $\chi_{\nu'}$ to the final-state χ_ν via the matrix elements

$$V_{\nu\nu'}=\langle\chi_\nu|\hat{V}|\chi_{\nu'}\rangle\ . \tag{9}$$

The FONDA approximation eliminates this significant computational complication.

B. The FONDA philosophy

The essential assumption underlying the FONDA approximation is separability of the electron-molecule wave function *in the entrance channel*: i.e., we replace ψ_0 in (7) by the product of the wave function for the *initial* rovibrational state of the target (ν_0) and an adiabatic electronic function which we denote ω_0:

$$\psi_0(\mathbf{r},\mathbf{R})\approx\omega_0(\mathbf{r};\mathbf{R})\chi_{\nu_0}(\mathbf{R})\ . \tag{10}$$

The scattering function ω_0 is adiabatic in that it depends *parametrically* on the molecular coordinates; it is in this important sense that (10) resembles the Born-Oppenheimer approximation of molecular structure theory.[34–36] Because this replacement is uniquely associated with the entrance channel, ω_0 corresponds unambiguously to the incident energy $k_0^2/2$. In particular, this function satisfies the single-particle scattering equation

$$(\hat{T}_e+\hat{V}-\tfrac{1}{2}k_0^2)\omega_0(\mathbf{r};\mathbf{R})=0\ . \tag{11}$$

Substitution of Eq. (10) into the exact inelastic amplitude (7) leads to an approximate amplitude *that is correct to first order in the interaction potential,*[11] viz.,

$$f_{\nu\nu_0}^{(1)}(\hat{\mathbf{r}})=\int\chi_\nu^*(\mathbf{R})\left[-(2\pi)^{1/2}\int e^{-i\mathbf{k}_{vj}\cdot\mathbf{r}'}\hat{V}(\mathbf{r}',\mathbf{R})\omega_0(\mathbf{r}';\mathbf{R})d\mathbf{r}'\right]\chi_{\nu_0}(\mathbf{R})d\mathbf{R}\ . \tag{12a}$$

The quantity in large parentheses in (12a) is an adiabatic scattering amplitude; denoting this quantity $\bar{f}_0(\hat{\mathbf{r}};\mathbf{R})$, we can write this equation as a matrix element with respect to the initial and final target states, i.e.,

$$f_{\nu\nu_0}^{(1)}(\hat{\mathbf{r}})=\langle\chi_\nu|\bar{f}_0(\hat{\mathbf{r}};\mathbf{R})|\chi_{\nu_0}\rangle\ . \tag{12b}$$

Structurally Eq. (12b) resembles the inelastic amplitude of canonical AN theory, but it differs from its AN counterpart in one crucial respect: $\bar{f}_0(\hat{\mathbf{r}};\mathbf{R})$ is an off-shell amplitude[37] and therefore correctly incorporates the energies of the exit channel (in the wave vector $\mathbf{k}_{vj}$) and the entrance channel (in the function ω_0).

Comparison of the exact amplitude (8) with its FONDA approximate (12a) reveals that the separability approximation (10) has transformed the coupling of the intermediate states ν' to the final state ν into a parametric dependence of the scattering function ω_0 on the coordinates of the nuclear geometry.[38]

Were we to further approximate Eqs. (12) by evaluating the adiabatic amplitude $\bar{f}_0$ on the energy shell (i.e., by setting $k_{vj}=k_0$), we would reduce the inelastic amplitude (12) to the AN amplitude, which is *second order* in the interaction potential.[11] Because the AN amplitude treats

the initial and final target states as degenerate, it violates the conservation of energy requirement (5).

The impact of this violation on the accuracy of the AN cross section depends on the proximity of the incident energy to the threshold and on the energy loss $\varepsilon_v - \varepsilon_0$ experienced by the electron as a consequence of the excitation. For example, the threshold for the $v_0=0\rightarrow v=1$ excitation in e-H_2 scattering is about 0.5 eV, while that for the pure rotational excitation $0\rightarrow 2$ is about 0.04 eV; correspondingly, the errors due to the AN approximation for vibration are far more severe and encompass a much wider range of energy than those for rotation.[20,21] Because the FONDA theory is based on an off-shell amplitude, it eliminates this source of error at the modest cost of requiring integration over the adiabatic electronic function in Eq. (12b).

C. Implementation for electron-molecule scattering

In practice, implementation of the FONDA formalism is complicated by the fact that the nonspherical potential $\hat{V}$ couples the rotational angular momentum of the target $\mathbf{j}$ and the orbital angular momentum of the projectile l so that neither is a constant of the motion. However, the square of the total angular momentum $\mathbf{J}=\mathbf{j}+l$ and its projection on the (LF) quantization axis $\hat{e}_z$ are constants of the motion, and it is extremely important in any practical collision theory to exploit the resulting invariance properties of the scattering matrix.

To do so we require a basis of eigenfunctions of $\hat{J}^2$, i.e., the coupled-angular-momentum (CAM) representation of LFCC theory.[8,9,39] Specifically, the CAM basis consists of eigenfunctions of $\hat{J}^2$, $\hat{J}_z$, $\hat{l}^2$, $\hat{j}^2$, and $\hat{\mathcal{H}}_m^{(v)}$. If we approximate the target eigenfunctions as products of spherical harmonics (to represent the rotational motion) and vibrational functions, i.e.,[40]

$$\chi_v(\mathbf{R})=\phi_v(R)Y_{jm_j}(\hat{\mathbf{R}}) , \tag{13}$$

then these basis functions are products of vibrational eigenfunctions ϕ_v and the coupled angular functions[41]

$$\mathcal{Y}_{jl}^{JM}(\hat{\mathbf{r}},\hat{\mathbf{R}})=\sum_{m_j,m_l} C(jlJ;m_j m_l M)Y_{jm_j}(\hat{\mathbf{R}})Y_{lm_l}(\hat{\mathbf{r}}) . \tag{14}$$

These angular functions are not separable in $\hat{\mathbf{r}}$ and $\hat{\mathbf{R}}$, so in the CAM formulation, projectile and target variables are inextricably mixed. This feature makes implementing a Born-Oppenheimer separation of those variables much less straightforward than in Eq. (10) of Sec. II B.

To recast the FONDA equations in the CAM representation we must introduce a wave function whose boundary conditions identify the entrance channel with energy $k_0^2/2$ and with initial quantum numbers l_0, m_{l_0}, and J. We cannot use the wave function $\psi_0(\mathbf{r},\mathbf{R})$ because its boundary conditions, Eq. (6), identify the entrance channel with the wave vector $\mathbf{k}_0$. But the desired function $\Psi^J_{v_0 j_0 l_0}$ is simply related to ψ_0, i.e.,

$$\psi_0(\mathbf{r},\mathbf{R})=\sum_J \sum_{l_0,m_{l_0}} C(j_0 l_0 J;m_{j_0} m_{l_0} M) \times c_{l_0 m_{l_0}}(\mathbf{k}_0)\Psi^J_{v_0 j_0 l_0}(\mathbf{r},\mathbf{R}) . \tag{15}$$

Here $C(j_0 l_0 J;m_{j_0} m_{l_0} M)$ is the Clebsch-Gordan coefficient appropriate to the entrance channel and

$$c_{l_0 m_{l_0}}(\mathbf{k}_0)=\langle k_0,l_0,m_{l_0}|\mathbf{k}_0\rangle = k_0^{-1/2}Y^*_{l_0 m_{l_0}}(\hat{\mathbf{k}}_0) \tag{16}$$

effects the necessary change of basis from plane-wave to angular momentum eigenstates.[42] The (exact) integral equation for the K matrix corresponding to $\Psi^J_{v_0 j_0 l_0}$ is

$$K^J_{vjl,v_0 j_0 l_0}=-\frac{2}{\sqrt{k_{vj}k_0}}\int \hat{j}_l(k_{vj}r)\phi^*_v(R)\mathcal{Y}^{JM*}_{jl}(\hat{\mathbf{r}},\hat{\mathbf{R}})\hat{V}(\mathbf{r},\mathbf{R})\Psi^J_{v_0 j_0 l_0}(\mathbf{r},\mathbf{R})d\mathbf{r}\,d\mathbf{R} , \tag{17}$$

where $\hat{j}_l(k_{vj}r)$ is the Riccati-Bessel function[33] evaluated at wave number k_{vj}.

1. The BF FN radial functions

In order to effect a parametrized separation of variables in the CAM representation, we call upon the solution of the electron-molecule Schrödinger equation in the fixed-nuclear-orientation approximation, which amounts to neglecting molecular rotations for the duration of the collision.[11,12,43] To facilitate the solution of this equation, one usually writes it in a body-fixed coordinate frame defined so that the polar axis is coincident with the internuclear axis. The axes of the BF are related to those of the LF via a simple Euler-angle rotation.[44]

We begin by defining a LF adiabatic electronic function $\omega_{l_0 m_{l_0}}(\mathbf{r};\mathbf{R})$ that obeys appropriate angular momentum boundary conditions [cf. Eq. (15)]. This function is related to the adiabatic function $\omega_0(\mathbf{r};\mathbf{R})$ of Eq. (10) by the transformation matrix (16), i.e.,[6]

$$\omega_0(\mathbf{r};\mathbf{R})=\sum_{l_0,m_{l_0}} c_{l_0 m_{l_0}}(\mathbf{k}_0)\omega_{l_0 m_{l_0}}(\mathbf{r};\mathbf{R}) . \tag{18}$$

We now expand $\omega_{l_0 m_{l_0}}(\mathbf{r};\mathbf{R})$ in partial waves so as to introduce LF radial scattering functions, viz.,

$$\omega_{l_0 m_{l_0}}(\mathbf{r};\mathbf{R})=\frac{1}{r}\sum_{l,m_l} u_{lm_l,l_0 m_{l_0}}(r;\mathbf{R})Y_{lm_l}(\hat{\mathbf{r}}) . \tag{19}$$

We can relate these LF radial functions to their BF counterparts via the Wigner rotation matrices,

$$u_{lm_l,l_0 m_{l_0}}(r;\mathbf{R})=\sum_\Lambda \mathcal{D}^l_{m_l\Lambda}(\hat{\mathbf{R}})u^\Lambda_{ll_0}(r;R)\mathcal{D}^{l_0*}_{m_{l_0}\Lambda}(\hat{\mathbf{R}}) . \tag{20}$$

The summation index Λ is the quantum number for the projection of l on the BF polar axis (the internuclear axis). It is important to note that, contrary to appearances, this rotation does not eliminate the crucial parametric dependence of the LF adiabatic scattering functions on $\hat{\mathbf{R}}$. This dependence does not, however, appear *explicitly* in the BF radial functions $u^{\Lambda}_{ll_0}(r;R)$ because the rotation (20) has transformed it into the sum over Λ.

2. *The FONDA CAM K matrix*

To develop the FONDA approximation to the LF CAM K matrix (17) we first factor out of $\Psi^J_{v_0 j_0 l_0}(\mathbf{r},\mathbf{R})$ the initial vibrational state function $\phi_{v_0}(R)$, viz.,

$$\Psi^J_{v_0 j_0 l_0}(\mathbf{r},\mathbf{R}) \approx \Omega^J_{j_0 l_0}(\mathbf{r},\hat{\mathbf{R}};R)\phi_{v_0}(R) , \tag{21}$$

where the multiplicative factor $\Omega^J_{j_0 l_0}$ depends parametrically on R. To separate the angular variables of rotational motion, we introduce CAM LF radial scattering functions by expanding the vibrationally adiabatic function $\Omega^J_{j_0 l_0}$ in the angular basis of Eq. (14),

$$\Omega^J_{j_0 l_0}(\mathbf{r},\hat{\mathbf{R}};R) = \frac{1}{r}\sum_{j',l'} u^J_{j'l',j_0 l_0}(r;R)\mathcal{Y}^{JM}_{j'l'}(\hat{\mathbf{r}},\hat{\mathbf{R}}) . \tag{22}$$

We approximate the rotational dynamics by replacing the LF function by appropriately transformed BF functions *in the fixed-nuclear-orientation approximation.* These are just the functions $u^{\Lambda}_{ll_0}$ of Eq. (20). But since the angular momenta are coupled in (22), we must relate these functions to the LF radial functions by a rotational frame transformation which simultaneously rotates the BF FN scattering function into the LF through Eq. (20) and transforms the rotated FN function into the CAM representation.[45,46] Like the simple rotation of Eq. (20), this transformation changes the parametric dependence of the LF CAM scattering function on $\hat{\mathbf{R}}$ into a sum over Λ:

$$u^J_{jl,j_0 l_0}(r;R) = \sum_{\Lambda} A^{jl}_{j\Lambda}\, u^{\Lambda}_{ll_0}(r;R)\, A^{jl_0}_{jl_0\Lambda} . \tag{23}$$

For a diatomic target the elements of this transformation are[4]

$$A^{jl}_{j\Lambda} = \left[\frac{2j+1}{2J+1}\right]^{1/2} C(jlJ;0\Lambda\Lambda) . \tag{24}$$

The LF CAM equivalent of the FONDA separation (10) is simultaneous application of (21) and (23). Introducing these separability approximations and the expansion (22) into the exact integral equation (17) for the LF CAM K matrix, we obtain an expression for the first-order approximation:

$$K^{J(1)}_{vjl,v_0 j_0 l_0} = -\frac{2}{\sqrt{k_{vj}k_0}}\int \hat{j}_l(k_{vj}r)\phi^*_v(R)\mathcal{Y}^{JM*}_{jl}(\hat{\mathbf{r}},\hat{\mathbf{R}})\hat{V}(\mathbf{r},\mathbf{R})\frac{1}{r}\sum_{j',l'}\left[\sum_{\Lambda} A^{jl'}_{j'\Lambda}u^{\Lambda}_{l'l_0}(r;R)A^{jl_0}_{j_0\Lambda}\right]\mathcal{Y}^{JM}_{j'l'}(\hat{\mathbf{r}},\hat{\mathbf{R}})\phi_{v_0}(R)d\mathbf{r}\,d\mathbf{R} . \tag{25}$$

Fortunately, this expression is amenable to considerable simplification. The integration over angular variables $\hat{\mathbf{r}}$ and $\hat{\mathbf{R}}$ introduces the rotational coupling matrix elements of conventional LF CAM theory,[9]

$$V^J_{jl,j'l'}(r,R) = \int \mathcal{Y}^{JM*}_{jl}(\hat{\mathbf{r}},\hat{\mathbf{R}})\hat{V}(\mathbf{r},\mathbf{R})\mathcal{Y}^{JM}_{j'l'}(\hat{\mathbf{r}},\hat{\mathbf{R}})d\hat{\mathbf{r}}\,d\hat{\mathbf{R}} . \tag{26}$$

But, like the radial functions in (23), these matrix elements are related to their BF counterparts by the rotational frame transformation (24),

$$V^J_{jl,j'l'}(r) = \sum_{\Lambda'} A^{jl}_{j\Lambda'}V^{\Lambda'}_{l,l'}(r)A^{jl'}_{j'\Lambda'} . \tag{27}$$

If we insert Eqs. (26) and (27) into Eq. (25), we can use the orthogonality of the rotational frame transformation to evaluate the sum over j' in (25) and then execute the sum over Λ' in (27). We obtain an equation for the K matrix that involves only radial integrals,

$$K^{J(1)}_{vjl,v_0 j_0 l_0} = \left\langle \phi_v \left| \sum_{\Lambda} A^{jl}_{j\Lambda}\left[-\frac{2}{\sqrt{k_{vj}k_0}}\int_0^{\infty}\hat{j}_l(k_{vj}r)\left[\sum_{l'}V^{\Lambda}_{l,l'}(r,R)u^{\Lambda}_{l'l_0}(r;R)\right]dr\right]A^{jl_0}_{j_0\Lambda}\right|\phi_{v_0}\right\rangle . \tag{28}$$

This form shows how the FONDA approximation transforms coupling of (all) intermediate rotational states j' to the final state j into a sum over Λ. The BF radial functions in the integrand in (28), which depend parametrically on R and, through $\sum_{\Lambda}$, on $\hat{\mathbf{R}}$,[47] solve the BF FN coupled radial integrodifferential equations for the "body energy" $k_b^2/2$,[6]

$$\left[\frac{d^2}{dr^2} - \frac{l(l+1)}{r^2} + k_b^2\right]u^{\Lambda}_{ll_0}(r;R) = 2\sum_{l'}V^{\Lambda}_{l,l'}(r,R)u^{\Lambda}_{l'l_0}(r;R) , \tag{29}$$

subject to the K-matrix boundary conditions

$$u^{\Lambda}_{ll_0} \underset{r\to\infty}{\sim} \delta_{ll_0}\hat{j}_{l_0}(k_b r) - K^{\Lambda}_{ll_0}(R)\hat{n}_l(k_b r) , \tag{30}$$

where $\hat{n}_l(k_b r)$ is the Riccati-Neumann function evaluated at the body wave number k_b.

Just as in the derivation of Sec. II A we wrote the FONDA scattering amplitude in terms of an off-shell amplitude in Eqs. (12), here we can write the FONDA CAM K matrix (28) in terms of the off-shell (FN) K matrix

$$\bar{K}^{\Lambda}_{ll_0}(k_{vj},k_0,R)\equiv\left[-\frac{2}{\sqrt{k_{vj}k_0}}\int_0^\infty \hat{j}_l(k_{vj}r)\left[\sum_{l'} V^{\Lambda}_{l,l'}(r,R)u^{\Lambda}_{l'l_0}(r;R)\right]dr\right] \tag{31}$$

as

$$K^{J(1)}_{vjl,v_0j_0l_0}=\left\langle\phi_v\left|\sum_{\Lambda} A^{Jl}_{j\Lambda}\bar{K}^{\Lambda}_{ll_0}(k_{vj},k_0,R)A^{Jl_0}_{j_0\Lambda}\right|\phi_{v_0}\right\rangle . \tag{32}$$

Because the energy of the BF radial functions is *unambiguously* identified with the entrance channel, i.e., $k_b^2/2=k_0^2/2$ in Eqs. (29), the FONDA approximation does not suffer from the ambiguity of definition of the BF energy that plagues AN theory.[5,48] More importantly, since the adiabatic K matrix in (31) is evaluated off the energy shell, the FONDA K matrix properly conserves energy according to Eq. (5).

Although the FONDA K matrix (28) depends only on the initial and final target wave functions, it is not merely an approximation to the reactance matrix of two-state close-coupling equations. Because it is based on a Born-Oppenheimer separation via Eqs. (21) and (23), this K matrix incorporates coupling to *all* intermediate states through its parametric dependencies on R and (in the sum over Λ) on $\hat{\mathbf{R}}$.

3. The (local) FONDA equations in a convenient form

We can write the FONDA K matrix for a local potential[49–51] in a form convenient for computation by introducing the Legendre projections $v_\lambda(r,R)$ of the (axially symmetric) potential,

$$V(\mathbf{r},R)=\sum_{\lambda} v_\lambda(r,R)P_\lambda(\cos\theta) . \tag{33}$$

In terms of these projections, the BF coupling matrix elements in (28) are simply

$$V^{\Lambda}_{l,l'}(r,R)=\sum_{\lambda} g_\lambda(ll';\Lambda)v_\lambda(r,R) \tag{34}$$

with coupling coefficients

$$g_\lambda(ll';\Lambda)=\left[\frac{2l'+1}{2l+1}\right]^{1/2}C(l'\lambda l;\Lambda 0)C(l'\lambda l;00) . \tag{35}$$

With these definitions we can write the radial integrals in Eq. (28) as

$$I^{\Lambda}_{l'\lambda}(k_{vj}ll_0;R)\equiv\int_0^\infty \hat{j}_l(k_{vj}r)v_\lambda(r,R)u^{\Lambda}_{l'l_0}(r;R)dr \tag{36}$$

and the FONDA approximation (28) to the LF CAM K matrix as

$$K^{J(1)}_{vjl,v_0j_0l_0}=-\frac{2}{\sqrt{k_{vj}k_0}}\sum_{\Lambda} A^{Jl}_{j\Lambda}\left[\sum_{l',\lambda} g_\lambda(ll';\Lambda)\langle\phi_v|I^{\Lambda}_{l'\lambda}(k_{vj}ll_0;R)|\phi_{v_0}\rangle\right]A^{Jl_0}_{j_0\Lambda} . \tag{37}$$

This form shows the steps one must carry out to evaluate the FONDA K matrix for a particular rovibrational excitation.

(i) Evaluate the frame transformation and coupling coefficients of Eqs. (35) and (24) in terms of Clebsch-Gordan coefficients.

(ii) Calculate the Legendre projections v_λ of the potential $\hat{V}$, here assumed to be local.[25]

(iii) Solve the BF FN coupled equations (29) for the electron-molecule symmetries required to converge the sums over Λ and l' in the K matrix (37); this step is simplified by the fact that except for very-low-order symmetries (e.g., $\Lambda\leq 1$ for e-H_2) one can trivially calculate the contributions to these sums using the unitarized Born approximation.[52]

(iv) Evaluate the FONDA radial integrals (36) via simple radial quadratures over r and R.

Because it completely eliminates coupling to intermediate target states, this method, although not quite as simple computationally as the AN approximation, requires far less computer time than a fully converged rovibrational close-coupling calculation.

4. Reduction of FONDA to AN theory

If we impose on the FONDA K matrix (32) the further approximation of target-state degeneracy (see Sec. II B) by setting $k_{vj}=k_0$ in the exit-channel wave function $\hat{j}_l(k_{vj}r)$, then the off-shell adiabatic K matrix (31) collapses onto the energy shell, where it becomes the K matrix of conventional BF FN theory,[4]

$$K^{\Lambda}_{ll_0}(R)=-\frac{2}{k_0}\int_0^\infty \hat{j}_l(k_br)\sum_{l'} V^{\Lambda}_{l,l'}(r,R)u^{\Lambda}_{l'l_0}(r;R)dr , \tag{38}$$

evaluated at the incident wave number $k_b=k_0$. Correspondingly, the FONDA K matrix becomes the (second-order) K matrix of conventional AN theory,

$$K^{J(2)}_{vjl,v_0j_0l_0}=\sum_{\Lambda} A^{Jl}_{j\Lambda}\langle\phi_v|K^{\Lambda}_{ll_0}(R)|\phi_{v_0}\rangle A^{Jl_0}_{j_0\Lambda} . \tag{39}$$

This reduction shows that in the hierarchy of electron-molecule collision theories, the FONDA K matrix (37) sits between the exact LF CAM K matrix of Eq. (17) and the AN approximation to this matrix, Eq. (39).

D. FONDA Theory with nonlocal potentials

A rigorous representation of the electron-molecule interaction includes two kinds of nonlocal terms: exchange potentials and bound-free correlation potentials. (The latter arise because certain two-particle Coulomb interactions are neglected in a one-electron treatment.) Strictly

speaking, then, the potential $\hat{V}$ in the reduced Schrödinger equation (1) is the sum of local electrostatic and polarization terms and nonlocal exchange and correlation terms. The nonlocal potentials are integral operators that, like the local terms, couple both partial waves and target states.

Much of the development in Sec. II B leading to the FONDA LF CAM K matrix (37) applies whether or not the potential $\hat{V}$ contains nonlocal terms. But if present, nonlocal terms give rise to an additional K matrix that must be added to the local matrix (37). In this section we show how to modify the FONDA method if nonlocal potentials are present by using as a specific case the exchange operator $\hat{V}_{ex}$. As in previous subsections, we first modify the simple scattering amplitude of Eqs. (7) and (8), then the LF CAM K matrix (17).

1. The FONDA nonlocal scattering amplitude

If $\hat{V}$ contains a nonlocal term $\hat{V}_{ex}$, then the coupling matrix element in the exact scattering amplitude (8) consists of two terms: a local element, which simply multiplies the channel functions $\zeta_{\nu'\nu_0}(\mathbf{r}')$, and a nonlocal element, which acts on these functions as an integral operator, i.e.,

$$\hat{V}_{\nu\nu'}(\mathbf{r}')\zeta_{\nu'\nu_0}(\mathbf{r}')=\int \mathcal{H}_{\nu\nu'}(\mathbf{r}',\mathbf{r}'')\zeta_{\nu'\nu_0}(\mathbf{r}'')d\mathbf{r}'' \ . \tag{40}$$

The function $\mathcal{H}_{\nu\nu'}$ is the matrix element between target states χ_ν and $\chi_{\nu'}$ of the exchange kernel $\mathcal{H}(\mathbf{r}',\mathbf{r}'')$, which, in turn, is defined in terms of the N_{occ} Born-Oppenheimer occupied molecular orbitals ξ_i of the target as

$$\mathcal{H}(\mathbf{r}',\mathbf{r}'')=-\sum_{i=1}^{N_{occ}}\xi_i(\mathbf{r}';R)\frac{1}{|\mathbf{r}'-\mathbf{r}''|}\xi_i^*(\mathbf{r}'';R) \ . \tag{41}$$

The exact *exchange amplitude* for an electron with outgoing wave vector $\mathbf{k}_{\nu j}=k_{\nu j}\hat{\mathbf{r}}$ has the form

$$f_{\nu\nu_0}(\hat{\mathbf{r}})|_{ex}=-(2\pi)^{1/2}\int\int e^{-i\mathbf{k}_{\nu j}\cdot\mathbf{r}'}\sum_{\nu'}\mathcal{H}_{\nu\nu'}(\mathbf{r}',\mathbf{r}'')\zeta_{\nu'\nu_0}(\mathbf{r}'')d\mathbf{r}'d\mathbf{r}'' \ , \tag{42}$$

where to avoid clutter we have suppressed the dependence of the exchange kernel and its matrix elements on $\mathbf{R}$.

To develop the FONDA approximation to this amplitude, we insert the exchange matrix elements into (42) and apply the FONDA separation (10), obtaining

$$f^{(1)}_{\nu\nu_0}(\hat{\mathbf{r}})|_{ex}=\int\chi_\nu^*(\mathbf{R})\left[-(2\pi)^{1/2}\int\int e^{-i\mathbf{k}_{\nu j}\cdot\mathbf{r}'}\mathcal{H}(\mathbf{r}',\mathbf{r}'')\omega_0(\mathbf{r}'';\mathbf{R})d\mathbf{r}'d\mathbf{r}''\right]\chi_{\nu_0}(\mathbf{R})d\mathbf{R} \ . \tag{43}$$

The full FONDA scattering amplitude is just the sum of Eqs. (12a) for the direct potential and (43) for the exchange term.

In practice, evaluation of the exchange amplitude is complicated by the sixfold integral over the projectile coordinates. By expanding the adiabatic scattering function $\omega_0(\mathbf{r}'';\mathbf{R})$ in partial waves we can reduce this to a twofold integral over r' and r''—but evaluating even this integral is quite time consuming.

We can greatly simplify this calculation by representing the kernel on a basis of orthogonal $\mathcal{L}^2$ functions $\bar{\eta}(\mathbf{r})$ which diagonalize it.[53] In practice, we choose these basis functions from the bound and virtual molecular orbitals of the molecule, which we construct as symmetry-adapted linear combinations of multicenter Cartesian Gaussians (see Sec. III).[54]

We write the resulting separable representation of the exchange kernel in terms of these basis functions and the kernel eigenvalues κ_γ as

$$\mathcal{H}(\mathbf{r}',\mathbf{r}'')=\sum_\gamma\bar{\eta}_\gamma^*(\mathbf{r}';R)\kappa_\gamma(R)\bar{\eta}_\gamma(\mathbf{r}'';R) \ . \tag{44}$$

All of the quantities in Eq. (44) depend on the internuclear separation and thus participate in the integral over R in the matrix element (43).

Introducing this separable representation into the first-order amplitude (43) transforms the off-shell amplitude (the quantity in square brackets) into the product of two single-variable integrals, viz.,

$$f^{(1)}_{\nu\nu_0}(\hat{\mathbf{r}})|_{ex}=\int\chi_\nu^*(\mathbf{R})\left[-(2\pi)^{1/2}\sum_\gamma\kappa_\gamma(R)\left[\int e^{-i\mathbf{k}_{\nu j}\cdot\mathbf{r}'}\bar{\eta}_\gamma^*(\mathbf{r}';R)d\mathbf{r}'\right]\left[\int\bar{\eta}_\gamma(\mathbf{r}'';R)\omega_0(\mathbf{r}'';\mathbf{R})d\mathbf{r}''\right]\right]\chi_{\nu_0}(\mathbf{R})d\mathbf{R} \ . \tag{45}$$

Subsequent expansion of ω_0 in partial waves reduces each integral in (45) to a single radial integral. Because the exchange basis $\{\bar{\eta}_\gamma\}$ consists of $\mathcal{L}^2$ functions, these integrals are short range and can be evaluated with a simple radial quadrature.[55] Alternatively, the first integral in large parentheses in (45) can be evaluated in closed form provided the exchange basis functions are expressed as a linear combination of Cartesian Gaussians.[56]

2. The FONDA nonlocal K matrix in the CAM representation

The derivation of FONDA LF CAM exchange K matrix begins with Eq. (17) for the exact integral equation, with $\hat{V}$ replaced by the exchange potential $\hat{V}_{ex}$, and proceeds as in Sec. II C 2 until Eq. (25). In the next step, which relates the LF CAM matrix elements to BF coupling matrix elements via the rotational frame transfor-

mation, we must allow for the nonlocal effect of the LF matrix elements on the (fixed-R) radial scattering functions, i.e.,

$$\hat{\mathcal{V}}^J_{jl,j'l'}(r)u^J_{j'l',j_0l_0}(r;R) = \int \mathcal{K}^J_{jl,j'l'}(r,r')u^J_{j'l',j_0l_0}(r';R)dr' , \quad (46)$$

where the (fixed-R) LF CAM exchange kernel is[10]

$$\mathcal{K}^J_{jl,j'l'}(r',r'') = -r'r''\langle \mathcal{Y}^{JM}_{jl}|\mathcal{K}(\mathbf{r}',\mathbf{r}'')|\mathcal{Y}^{JM}_{j'l'}\rangle \quad (47)$$

and the matrix element in (47) implies integration over $\hat{\mathbf{r}}'$, $\hat{\mathbf{r}}''$, and $\hat{\mathbf{R}}$.

The LF CAM exchange matrix element in (46) transforms under the rotational frame transformation (24) just like its local counterpart in Eq. (27). This transformation introduces the BF FN kernel $\mathcal{K}^{\Lambda}_{ll'}$, which is just the matrix representation of $\mathcal{K}(\mathbf{r}',\mathbf{r}'')$ in an angular momentum basis with quantization axis $\hat{\mathbf{R}}$, i.e.,

$$\mathcal{K}^{\Lambda}_{ll'}(r',r'') = -r'r''\int\int Y^*_{lm_l}(\hat{\mathbf{r}}')\mathcal{K}(\mathbf{r}',\mathbf{r}'')Y_{l'm_l}(\hat{\mathbf{r}}'')d\hat{\mathbf{r}}'d\hat{\mathbf{r}}'' . \quad (48)$$

The resulting FONDA CAM exchange K matrix structurally resembles the local form (28) but contains a double radial integral over the BF FN scattering functions [see Eq. (43)],

$$K^{J(1)}_{vjl,v_0j_0l_0}|_{\rm ex} = \left\langle \phi_v \left| \sum_{\Lambda} A^{Jl}_{j\Lambda} \left[-\frac{2}{\sqrt{k_{vj}k_0}} \sum_{l'} \int_0^{\infty}\int_0^{\infty} \hat{j}_l(k_{vj}r)\mathcal{K}^{\Lambda}_{ll'}(r,r')u^{\Lambda}_{l'l_0}(r';R)dr\,dr' \right] A^{Jl_0}_{j_0\Lambda} \right| \phi_{v_0} \right\rangle . \quad (49)$$

To simplify the double radial integral in Eq. (49) to a product of two short-range integrals as in Eq. (45), we represent the kernel on the $\mathcal{L}^2$ exchange basis $\{\bar{\eta}_\gamma(\mathbf{r};R)\}$. If we expand these basis functions in Legendre polynomials, and denote the resulting projections by $\bar{\eta}_{\gamma l}(r;R)$, we can write the (fixed-R) nonlocal BF exchange matrix element (48) as

$$\mathcal{K}^{\Lambda}_{ll'}(r,r') = \sum_{\gamma} \bar{\eta}^*_{\gamma l}(r;R)\kappa_\gamma(R)\bar{\eta}_{\gamma l'}(r';R) . \quad (50)$$

3. *The (nonlocal) FONDA equations in a convenient form*

Inserting Eq. (50) into Eq. (49) leads to a form for the exchange K matrix that is analogous to (37) for the local K matrix. We define radial integrals akin to the local integral (36),

$$X^{\Lambda}_{\gamma}(k_{vj}l;R) \equiv \int_0^{\infty} \hat{j}_l(k_{vj}r)\bar{\eta}^*_{\gamma l}(r;R)dr , \quad (51a)$$

$$Z^{\Lambda}_{\gamma l'}(k_0l_0;R) \equiv \int_0^{\infty} \bar{\eta}_{\gamma l'}(r;R)u^{\Lambda}_{l'l_0}(r;R)dr , \quad (51b)$$

and write Eq. (49) in the convenient form

$$K^{J(1)}_{vjl,v_0j_0l_0}|_{\rm ex} = -\frac{2}{\sqrt{k_{vj}k_0}} \sum_{\Lambda} A^{Jl}_{j\Lambda} \sum_{l',\gamma} \langle \phi_v|\kappa_\gamma(R)X^{\Lambda}_{\gamma}(k_{vj}l;R)Z^{\Lambda}_{\gamma l'}(k_0l_0;R)|\phi_{v_0}\rangle A^{Jl_0}_{j_0\Lambda} . \quad (52)$$

Our final result, the FONDA approximation to the LF CAM K matrix for a potential that includes local and nonlocal terms, is just the sum of (52) and its local counterpart (37),

$$K^{J(1)}_{vjl,v_0j_0l_0} = -\frac{2}{\sqrt{k_{vj}k_0}} \sum_{\Lambda} A^{Jl}_{j\Lambda} \sum_{l'} \left[\sum_{\lambda} g_\lambda(ll';\Lambda)\langle \phi_v|I^{\Lambda}_{l'\lambda}(k_{vj}ll_0;R)|\phi_{v_0}\rangle + \sum_{\gamma} \langle \phi_v|\kappa_\gamma(R)X^{\Lambda}_{\gamma}(k_{vj}l;R)Z^{\Lambda}_{\gamma l'}(k_0l_0;R)|\phi_{v_0}\rangle \right] A^{Jl_0}_{j_0\Lambda} . \quad (53)$$

In Sec. IV we use this K matrix to calculate differential and integral cross sections for e-H_2 collisions.

III. THE INTERACTION POTENTIAL AND COMPUTATIONAL DETAILS

In Sec. IV we consider three cases: rotational excitation from a local potential, rotational excitation from a nonlocal potential (both in the rigid-rotor approximation), and vibrational excitation from a local potential. This section describes parameters and potentials used in these cases.

A. Numerical considerations

To ensure that differences between cross sections from calculations based on different scattering theories actually reflect physical features that distinguish those theories, we must require a level of numerical accuracy of 1% or better in the solution of the scattering equations, calculation of integrals, and evaluation of cross sections.

In addition, we independently verify our FONDA calculations in two ways. First, we numerically reduce the off-shell FN K matrix (31) to its on-shell BF FN counterpart (38) which we can independently compute by solving Eqs. (29) subject to the boundary conditions (30). To do

so we just evaluate the off-shell FN K matrix (31) with the exit-channel energy $k_{vj}^2/2$ artificially set equal to the entrance-channel energy $k_0^2/2$. (For studies of vibrational excitation, we perform this check for several internuclear separations.) We find agreement to three or more decimal places in all elements of the K matrix that make significant contributions to differential or integrated cross sections.

Second, we artificially reproduce AN cross sections in a FONDA calculation by modifying the FONDA code to implement the additional approximation of target-state degeneracy by setting $k_{vj}=k_0$ in all integrals in Eq. (28). The resulting "pseudo-AN" cross sections agree with those from independent AN calculations to better than 1% at all energies.

B. The e-H_2 potentials

In several recent papers we have described in detail the static, local model exchange, and correlation/polarization potentials used in this work.[3,20,57] So here we shall merely summarize salient features of these potentials. All are based on a Hartree-Fock representation[58] of the ground electronic state of H_2. Thus we write the $X\,^1\Sigma_g^+$ wave function as a Slater determinant of symmetry-adapted molecular orbitals. For the static and model-exchange potentials we calculate these orbitals using a $(5s2p/3s2p)$ basis of contracted nucleus-centered Cartesian Gaussian functions.[59,60] The equilibrium ($R=1.402a_0$) electronic energy for the ground state of H_2 in this basis is $-1.132\,895E_h$, which is quite close to the HF limit[61] of $-1.133\,63E_h$. The quadrupole moment averaged over the ground vibrational state is $0.4704ea_0^2$, which compares favorably to the experimental value[62] of $0.474\pm0.034ea_0^2$.

The local model exchange potential is based on a free-electron-gas approximation for the target represented by this HF charge density.[49] The mathematical form of this potential contains a parameter I which is usually equated to the ionization potential of the target; to improve on the free-electron-gas approximation for the (two-electron) H_2 molecule, we choose this parameter at each internuclear separation so that model-exchange eigenphase sums in the Σ_u symmetry at 0.54 eV are equal to those from an exact exchange BF FN calculation; this determination is carried out at the static-exchange level.[50,63] We use the resulting $I(R)$ for all symmetries and all energies; no further adjustment is performed.

The correlation/polarization potential is based on a $(6s3p/4s3p)$ basis that is quite similar to the aforementioned $(5s2p/3s2p)$ basis but that includes additional s-type and p-type diffuse functions to allow for polarization distortions of the neutral charge cloud.[64,57] With this basis we perform variational calculations of the polarized and unpolarized energies and compute the polarization potential as the difference of these energies; in evaluating the two-electron bound-free integrals for this calculation we further implement a nonpenetrating approximation to allow for nonadiabatic effects.[65] The resulting potential includes adiabatic polarization effects exactly.

Asymptotically this potential reduces to a simple analytic function of the H_2 polarizability tensor, which therefore can be used to assess the accuracy of at least its long-range form. Evaluating this tensor at each R and averaging the result over the ground vibrational state, we obtain $5.376a_0^3$ and $1.410a_0^3$ for the spherical and nonspherical components of the polarizability tensor, respectively. The experimental values of these quantities[66,67] are $5.4265a_0^3$ and $1.3567a_0^3$.

In calculations where exchange effects are included via the nonlocal operator $\hat{V}_{ex}$, we use the separable repreentation described in Sec. II D [see Eq. (44)]. Essential to this representation is the choice of the symmetry-adapted $\hat{\mathcal{L}}^2$ functions that will represent the kernel. Figuring out how to construct this "exchange basis" for inelastic collisions is neither simple nor obvious, for although the kernel is compact, it is not governed by a stationary principle. To keep our focus here on the FONDA method, we simply present our exchange basis, deferring further discussion to a future publication.[68]

The exchange basis functions $\bar{\eta}_\gamma(\mathbf{r})$ in Eqs. (44)–(52) diagonalize the kernel. But for an arbitrary exchange basis $\{\eta_\gamma(\mathbf{r})\}$ this operator is not diagonal; instead its separable form is

$$\mathcal{K}(\mathbf{r},\mathbf{r}')=\sum_{\alpha,\beta}\eta_\alpha^*(\mathbf{r})K_{\alpha\beta}\eta_\beta(\mathbf{r}')\ . \tag{54}$$

In practice we diagonalize the matrix $K_{\alpha\beta}$ to obtain the functions $\bar{\eta}_\gamma(\mathbf{r})$ and the eigenvalues $\kappa(R)$ which appear in Eq. (44). All quantities in Eq. (54) depend on the (suppressed) internuclear separation R.

We construct our e-H_2 exchange basis from the set of normalized multicenter Cartesian Gaussian functions in Table I. This set includes "compact" functions (centered on the nuclei) that span the region of the target charge cloud and "diffuse" functions (centered on the center of mass of the molecule) that span the fringes of the charge cloud. (A highly accurate representation of both regions is essential for separable representations of exchange in inelastic scattering calculations.) The basis in Table I yields 14 Σ_g functions, 14 Σ_u functions, 9 Π_g functions, and 11 Π_u functions.

C. The local FONDA K matrix

Once the potential is specified and the solution of the BF FN scattering equations completed, calculation of the FONDA LF CAM K matrix for a local potential requires only evaluation of the radial integrals (36). For this purpose we use a simple Numerov integrator[69] with a maximum propagation radius of $130a_0$.

These integrals are then put into sums over Λ, l', and λ in the final expression for the FONDA K matrix, Eq. (37). For e-H_2 we achieve the desired 1% convergence by including $\Lambda=0$, 1, and 2 (i.e., all Σ, Π, and Δ symmetries), five partial waves l', and Legendre projections of the potential for $\lambda=0$, 2, 4, and 6. (Only even values of λ contribute because H_2 is homonuclear.)

Having determined the FONDA K matrix, there remains only calculation of cross sections from the corresponding LF CAM transition matrix $T^J_{vjl,v_0j_0l_0}$. In the total integrated cross section[4]

TABLE I. Basis set for separable exchange potential: primitive Cartesian Gaussian functions of the form $\eta_k(n,l,m,\zeta;\mathbf{r})=N_n(\zeta)r^{n-1}e^{-\zeta_k r^2}Y_l^m(\hat{\mathbf{r}})$.

Nucleus-centered functions					
l	ζ (units of a_0^{-1})	l	ζ (units of a_0^{-1})	l	ζ (units of a_0^{-1})
s	33.6444[a]	p	2.2284	d_{xy}	1.6
	5.057 96[a]		1.1[b]		0.8
	2.5		0.5184		0.4
	1.146 8		0.25[a]		0.2
	0.6		0.12		0.1
	0.321 144		0.04		0.05
	0.101 309	0.013[b]			
	0.04			d_{xz},d_{yz}	0.4
	0.02				0.13
"Diffuse" functions (center-of-mass)					
l	ζ (units of a_0^{-1})	l	ζ (units of a_0^{-1})	l	ζ (units of a_0^{-1})
s	0.06	p_x,p_y	0.04	d_{xy}	0.1
	0.024		0.013		0.04
		p_z	0.06		
			0.024		

[a]Contractions coefficients 0.123 884 24 and 0.926 094 96, respectively.
[b]GTO's of p_x and p_y type only.

$$\sigma_{v_0j_0\to vj}=\frac{\pi}{k_0^2(2j_0+1)}\sum_{l,l_0}(2J+1)|T^J_{vjl,v_0j_0l_0}|^2\ , \quad (55)$$

we include $J=0,1,\ldots,8$ and five partial waves. In the differential cross section[70]

$$\left.\frac{d\sigma}{d\Omega}\right|_{v_0j_0\to vj}=\frac{1}{4k_0^2}\sum_{\lambda'=0}^{\infty}A_{\lambda'}(v_0j_0\to vj)P_{\lambda'}(\cos\theta)\ , \quad (56)$$

this is not enough partial waves to achieve convergence at all angles. So we use the first Born approximation to complete the partial-wave sums to the desired convergence criteria.[71]

To calculate vibrational excitation cross sections we must perform the quadrature over R in the FONDA K matrices (37) and, if the potential contains nonlocal terms, in (52). For many systems, the vibrational wave functions $\phi_v(R)$ in these integrals can be approximated accurately by eigenfunctions of a simple harmonic oscillator.[40] For H_2, however, this approximation does not represent the ground-state electronic potential to sufficient accuracy, so we solve the nuclear Schrödinger equation numerically with the $X\,^1\Sigma_g^+$ electronic energy from the aforementioned Hartree-Fock calculations. We then perform the integral over R using a simple Gauss-Hermite quadrature.[72]

D. The scattering equations for nonlocal potentials

In FONDA calculations based on a separable representation of the exchange kernel, one additional technical matter arises. The BF FN equations (29) which one must solve for the radial functions in the FONDA integrals $I^{\Lambda}_{l'\lambda}(k_{vj}ll_0;R)$ and $Z^{\Lambda}_{\gamma l'}(k_0l_0;R)$ are now integro-differential equations, because the coupling matrix elements $V^{\Lambda}_{l,l'}(r,R)$ contain a nonlocal integral operator like the one in Eq. (46).

Fortunately a variety of numerical methods for solving these equations have been implemented and tested.[73,74] Because of its stability and suitability for supercomputer calculations, we use the linear algebraic algorithm of Schneider and Collins.[75] In this method one first transforms the BF FN equations into integral equations then imposes quadrature schemes on all integrals to further transform these equations into a set of simultaneous linear algebraic equations which can be solved using standard computer programs for matrix operations. For e-H_2 we require the BF FN radial functions only for $r<50a_0$; beyond this radius the potential is local, and we can trivially solve Eqs. (29) using the Numerov algorithm.

The BF FN radial function appears in the additional FONDA integrals (51). Both these integrals are short range, because the exchange basis functions are square integrable. We evaluate these integrals using Simpson's rule algorithm to a maximum radius of $30a_0$.

IV. RESULTS

A. Rotational excitation by a local potential

In this subsection we compare T-matrix elements and cross sections for rotational excitation of H_2 as calculated using various scattering theories. The context for these comparisons is the rigid-rotor approximation, with the internuclear separation of H_2 fixed at the equilibrium value $R_e=1.402a_0$, and the local-exchange approximation described in Sec. III. These simplifications permit calculation of LFCC quantities which serve as benchmarks for evaluating approximate theories.

1. Threshold behavior of the transition matrix

Near-threshold inelastic cross sections are determined by only a few elements of the LF CAM T matrix. For ex-

ample, very near the 0.044-eV threshold for the pure rotational excitation $j_0=0\rightarrow j=2$ in hydrogen, 85% of the integrated cross section comes from the single term in Eq. (55) with $l=0$, $l_0=2$, and $J=2$. Accurate calculation of near-threshold cross sections is therefore possible only if these critical T-matrix elements obey the correct threshold law.

Rigorously, the threshold behavior of each element of the LF CAM T matrix is controlled by the quantum number l of the outgoing electron as[6,20,76]

$$T^J_{vjl,v_0j_0l_0}\sim k_{vj}^{l+1/2} \text{ as } k_{vj}\rightarrow 0\ . \tag{57}$$

For example, the T-matrix element for $l=0$, $l_0=2$, and $J=2$, which is critical to $\sigma_{0\rightarrow 2}$, should approach zero as $k_{vj}^{1/2}$.

In Fig. 2(a) we examine the threshold behavior of this matrix element for several scattering theories. Since the LFCC theory treats the nuclear dynamics exactly, it produces a T matrix whose elements do obey this law. The

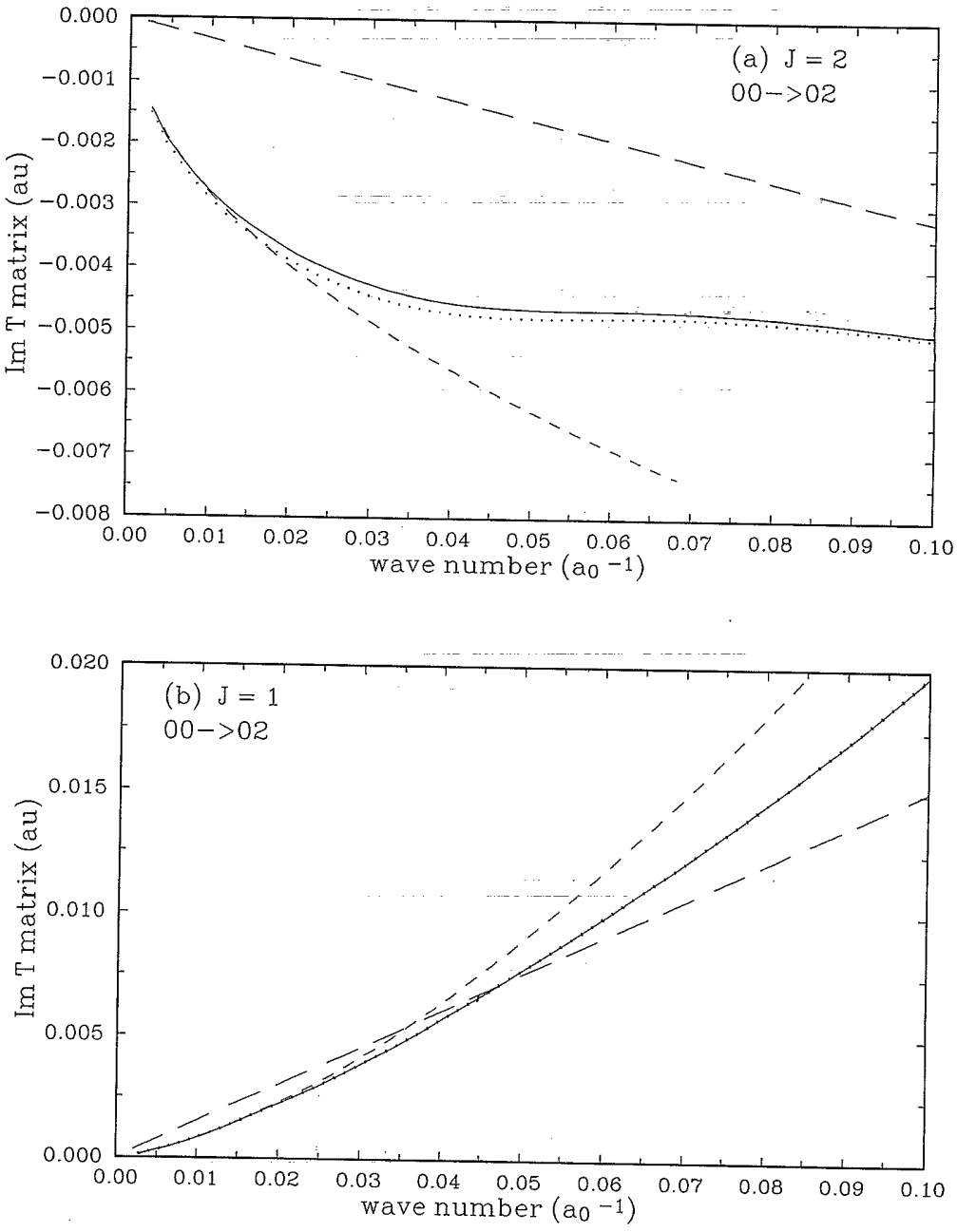

FIG. 2. The imaginary part of key transition matrix elements $T^J_{vjl,v_0j_0l_0}$ for the pure rotational excitation $0\rightarrow 2$: (a) total angular momentum $J=2$, entrance-channel angular momentum $l_0=0$, and exit channel angular momentum $l=2$; (b) $J=1$, $l_0=1$, and $l=1$. Various theories are compared to the threshold laws these matrix elements should obey (short-dashed curves): LFCC (solid curves), AN (long-dashed curves), and FONDA (dotted curves). The matrix elements in (a) should go to zero as $k_j^{5/2}$ and those in (b) as $k_j^{3/2}$.

FONDA method also produces the correct threshold dependence because it is based on an off-shell scattering matrix and conserves energy. The AN matrix elements, however, do not exhibit the correct dependence on k_j. Their low-energy behavior is controlled not by Eq. (57) but rather by the threshold law for the BF FN T matrix.

This threshold law of BF FN theory mirrors the long-range form of the interaction potential. If we specify the LF scattering angle θ by choosing the LF z axis along the incident direction $\hat{\mathbf{k}}_0$, then in the asymptotic region this potential reduces to a sum of terms of the form $r^{-s_\lambda}P_\lambda(\cos\theta)$. For a homonuclear target, the dominant long-range terms arise from[4,30] the quadrupole ($\lambda=2$, $s_2=3$) and (induced) polarization ($\lambda=0,2$, $s_0=s_2=4$) interactions.

Each such term gives rise to the following threshold behavior in the BF FN T-matrix elements[77]

$$T^A_{ll_0} \sim \begin{cases} k_b^{s_\lambda-2}, & l+l_0 > s_\lambda-3 \\ k_b^{l_0+l+1}, & l+l_0 \le s_\lambda-3 \end{cases}, \tag{58}$$

where k_b is the body wave number $k_b=\sqrt{2E_b}$. Since the BF FN wave function is independent of the state of the target, *this T matrix does not discriminate between the entrance and exit channels.* This defect is the source of the incorrect threshold behavior in Fig. 2.

In e-H_2, the quadrupole interaction, which is proportional to r^{-3}, dominates the polarization interaction, which is proportional to r^{-4}. Therefore all elements of the BF FN T matrix are simply proportional to the body wave number

$$T^\Lambda_{ll_0} \to k_b, \quad \text{as } k_b \to 0 . \tag{59}$$

In AN theory, this wave number is equal to the incident wave number k_0.

The AN T matrix whose elements appear in Fig. 2 is simply the rotationally frame-transformed BF FN T matrix [see Eq. (23)]. Since the factors $A^{Jl}_{j\Lambda}$ are independent of energy, the AN T-matrix elements are also proportional to k_b and so do not obey the threshold law (57). That is, in the AN approximation, $\sigma_{0\to2}$ is oblivious to the existence of a threshold and approaches a nonzero constant at this wave number. (The threshold for the $j_0=0\to j=2$ excitation in hydrogen occurs at the body wave number of $0.057a_0^{-1}$.)

In a conventional AN calculation one forces the inelastic cross section to zero at threshold by multiplying it by the wave-number ratio k_j/k_0.[16] This *ad hoc* modification alters the threshold behavior of only those T-matrix elements with $l=0$; elements with $l>0$, which may contribute significantly to the cross section, still behave incorrectly. For example, at an energy 3 meV above the threshold for pure rotational excitation of H_2, the terms in Eq. (55) with $J=1$ and $l=l_0=1$ contribute 15% of $\sigma_{0\to2}$. As the energy increases from threshold, T-matrix elements with $l>0$ rapidly predominate in this cross section. Thus by 1.0 eV, the $l=0$ element contributes only 20%; instead, the dominant contributor to this cross section is the term with $J=1$, $l=1$, $l_0=1$, which produces 65% of its value. So the now-dominant matrix element should behave as $k_j^{3/2}$, as it does in the LFCC and FONDA theories but not in the AN or modified AN approximations [see Fig. 2(b)].

2. *Differential and integrated cross sections*

The differing threshold behaviors of elements of the T matrix in various formulations has a striking effect on differential cross sections. Figure 3 shows cross sections for $j_0=0\to j=2$ at three energies from calculations based on the LFCC, modified AN (i.e., multiplied by the aforementioned wave-number ratio), and FONDA theories. Very near threshold for this excitation, the dominance of matrix elements with $l=0$ causes this cross section to be essentially isotropic—behavior which is reproduced by all three theories. By 1.0 eV, a pronounced dip appears. This dip, which arises from subtle

TABLE II. e-H_2 rotational excitation cross sections (in units of a_0^2) for $j_0=0\to j=2$ with local exchange potential (based on a rotational constant of $B_0=59.31\ \text{cm}^{-1}$).

E (eV)	LFCC	FONDA	SANR	EMA	ANR (mod)[a]	ANR	FBA(q)[b]	FBA (qp)[c]
0.047	0.046	0.048	0.060	0.065	0.074	0.298	0.056	0.062
0.060	0.126	0.132	0.137	0.143	0.159	0.309	0.117	0.132
0.080	0.189	0.192	0.198	0.202	0.221	0.330	0.153	0.176
0.100	0.231	0.233	0.241	0.243	0.263	0.352	0.170	0.201
0.200	0.378	0.380	0.394	0.387	0.441	0.499	0.201	0.257
0.300	0.510	0.512	0.530	0.517	0.545	0.590	0.211	0.285
0.400	0.648	0.647	0.671	0.654	0.685	0.726	0.215	0.305
0.500	0.794	0.796	0.821	0.800	0.834	0.873	0.218	0.321
1.000	1.657	1.652	1.698	1.662	1.709	1.748	0.223	0.382
3.000	4.859	4.851	4.927	4.858	4.891	4.927	0.226	0.538
5.000	5.540	5.433	5.473	5.443	5.450	5.472	0.227	0.659
10.000	3.998	3.985	3.990	3.985	3.982	3.990	0.227	0.911

[a]AN cross section modified by multiplication by wave number ratio k_j/k_0.
[b]First Born approximation with quadrupole interaction only, using $q=+0.451\,74ea_0^2$.
[c]First Born approximation with quadrupole and polarization interactions, using $\alpha_2=1.305a_0^3$.

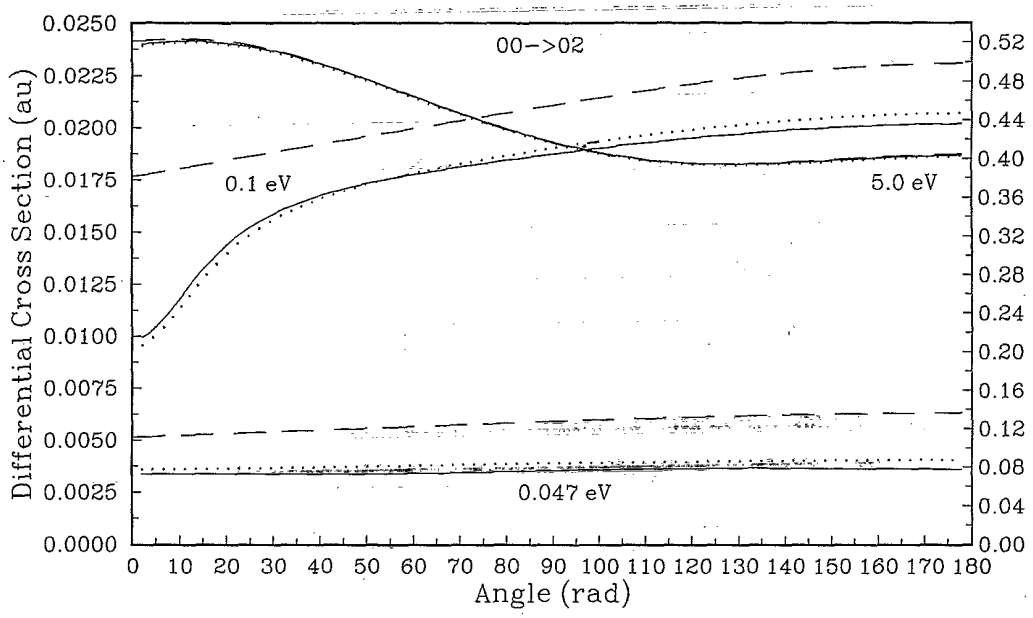

FIG. 3. Differential cross sections for the pure e-H_2 rotational excitation $0\rightarrow 2$ calculated with three scattering theories: LFCC (solid curve), AN (long-dashed curve), and FONDA (dots). Results are shown for 0.047, 0.1, and 5.0 eV. The scale on the right-hand axes pertains only to the 5.0-eV cross sections.

interference effects among different T-matrix element,[20] has recently been verified experimentally.[78] It appears only in the LFCC and FONDA cross sections. Finally by 5.0 eV, far from threshold, all three theories produce nearly identical cross sections.

Table II present values for $\sigma_{0\rightarrow 2}$ from LFCC, FONDA, AN, and modified AN calculations. We have also calculated this cross section using four other widely used theories. The first of these is the energy-modified approximation (EMA).[79] This method is usually implemented[20,80,48] by solving the BN FN scattering equations (29) with the body wave number set equal to the geometric mean for the excitation of interest, i.e., with $k_b=\sqrt{k_j k_0}$. Although this strategem does obviate the need for multiplication of the resulting cross section by k_j/k_0, it, like the AN method, corrects the threshold behavior only of T-matrix elements with $l=0$.

The second additional theory represented in Table II is the scaled adiabatic-nuclear-rotation (SANR) method.[81] This extremely simple procedure uses the first Born approximation to modify frame-transformed BF FN T matrices so as to ensure that *all* elements of this matrix obey the correct threshold law. Like the EMA, the SANR approximation also eliminates the need for *ad hoc* multiplication of inelastic cross section. Near threshold, the SANR procedure markedly improves inelastic integrated and differential cross sections. But with increasing energy, this method becomes theoretically dubious (because of its reliance on the Born approximation). Moreover it is not extensible to vibrational excitation.

The last two cross sections in Table II result from a first Born calculation using a potential consisting of either just the quadrupole interaction[82] or the sum of the quadrupole and induced-polarization interactions.[83] This is by far the simplest and most widely used procedure represented in this study. Unfortunately its treatment of both the interaction potential and the scattering dynamics is too crude to yield accurate results even near threshold.

To summarize, we present in Fig. 4 the percent differences for $j_0=0\rightarrow j=2$ as calculated in various approximate theories using the LFCC cross section as a standard. We find similar errors in the cross section for pure rotational excitation for other initial rotational states (e.g., $j=1$), for a potential that contains nonlocal terms (see Sec. IV B), and for calculations that include the vibrational dynamics.

B. Rotational excitation via a nonlocal exchange potential

Table III contains e-H_2 rotational-excitation cross sections calculated using the FONDA method with the non-

TABLE III. e-H_2 rotational excitation cross sections (in units of a_0^2) for $j_0=0\rightarrow j=2$ with nonlocal exchange. (See Table I for the exchange basis.)

E (eV)	Rigid rotor	Vibrationally averaged
0.047	0.065	0.070
0.060	0.133	0.149
0.080	0.194	0.212
0.100	0.233	0.255
0.200	0.368	0.539
0.300	0.488	0.678
0.400	0.612	0.990
0.500	0.746	1.347
1.000	1.562	1.743
3.000	5.064	5.584

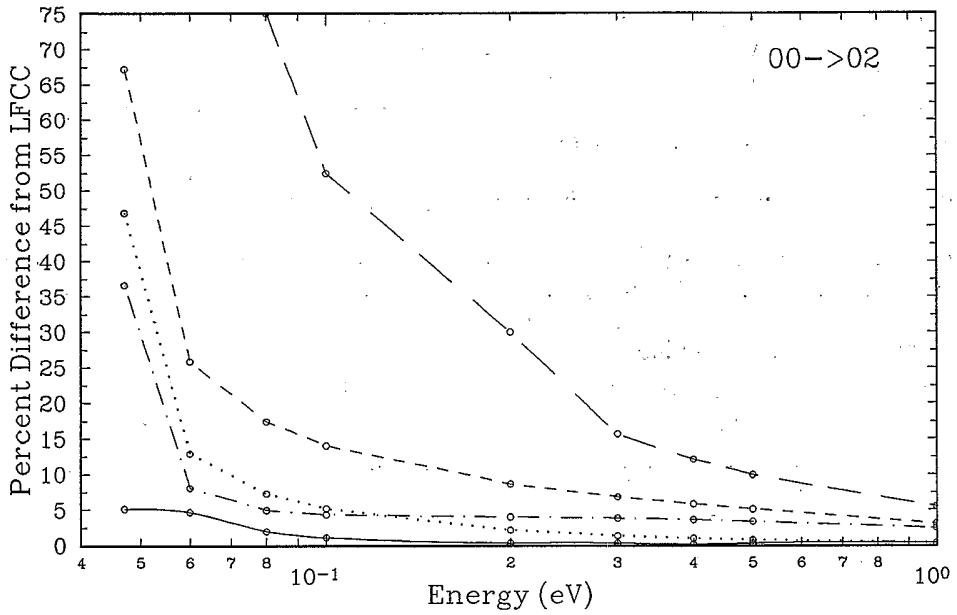

FIG. 4. Percent differences for the pure e-H_2 rotational excitation cross section $\sigma_{0\to 2}$ calculated using the LFCC result as a standard. Five approximate scattering theories are shown: AN (long-dashed curve), AN multiplied by k_j/k_0 (short-dashed curve), SANR (dot-dashed curve), EMA (dotted curve), and FONDA (solid curve). The open circles show the energies at which these comparisons were made.

local separable potential described in Sec. III B. These results differ little from the model-exchange cross sections in Table II, because our model potential is optimized for near-threshold rotational excitation.[20,57]

All cross sections presented so far have been calculated in the rigid-rotor approximation. But in the energy range from threshold to 10 eV this approximation introduces errors as large as 15% in this cross section.[84] By contrast, experimental determination of $\sigma_{0\to 2}$ (by solution of the Boltzmann equation for a swarm of electrons drifting

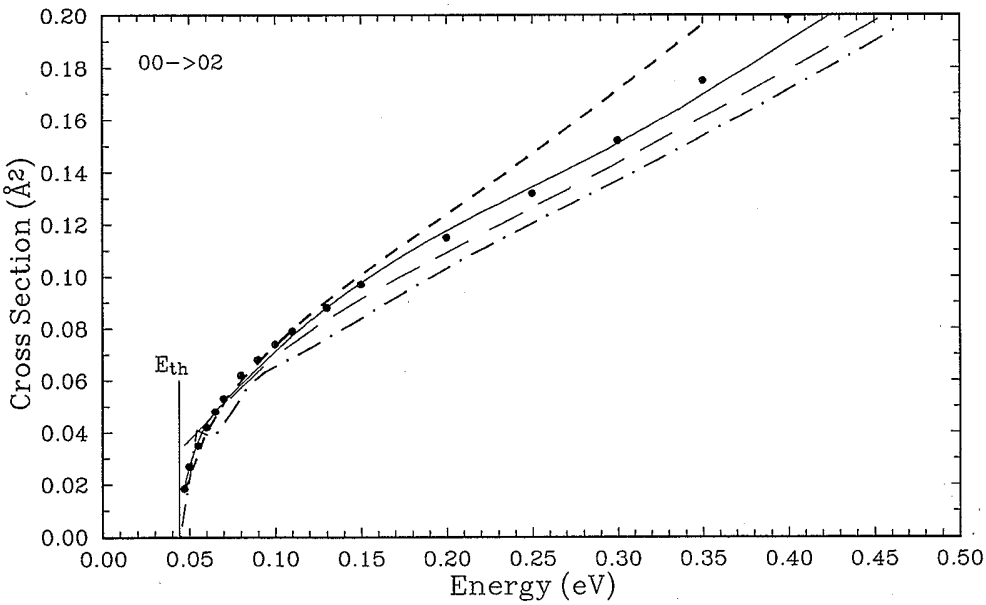

FIG. 5. Pure rotational excitation e-H_2 cross sections $\sigma_{0\to 2}$ calculated using various representations of exchange. Three of these cross sections are based on the separable representation of exchange described in Sec. III (see Table I): FONDA using a rigid-rotor potential (dot-dashed curve), FONDA using a vibrationally averaged potential (solid curve), and AN using a vibrationally averaged potential (long-dashed curve). The other cross section is calculated using the FONDA method with a vibrationally averaged potential that includes the local model exchange potential described in Sec. III (short-dashed curve). Also shown are experimental cross sections derived by transport analysis from electron swarm data (solid circles) and the threshold for this excitation (vertical line), 0.044 eV.

and diffusing through a gas under the influence of an applied external field) yields values accurate to a few percent at and below 1.5 eV.[3,85] So however accurate the representation of exchange and the rotational dynamics may be, rigid-rotor cross sections are inadequate for comparison to measured values.

To correct the rigid-rotor approximation, we have recently proposed an extremely simple procedure that restores the zero-point motion of the target for vibrationally elastic processes and eliminates almost all of the aforementioned error.[84] This vibrational averaging procedure entails simply replacing the equilibrium interaction potential in the BF FN matrix elements in (29) by the average of this potential over the ground vibrational state of the target,

$$V(\mathbf{r};R_e)\rightarrow\langle\phi_{v_0}(R)|V(\mathbf{r},R)|\phi_{v_0}(R)\rangle\ . \tag{60}$$

Using VIBAV static and polarization potentials and the (equilibrium) separable exchange potential of Sec. III C and Table I in a FONDA calculation, we obtain the rotational-excitation cross section in Table III and Fig. 5. This cross section agrees extremely well with the swarm-derived results. (We find comparable agreement for $\sigma_{1\rightarrow3}$.) By comparing these cross sections with results from various other formulations, this figure also

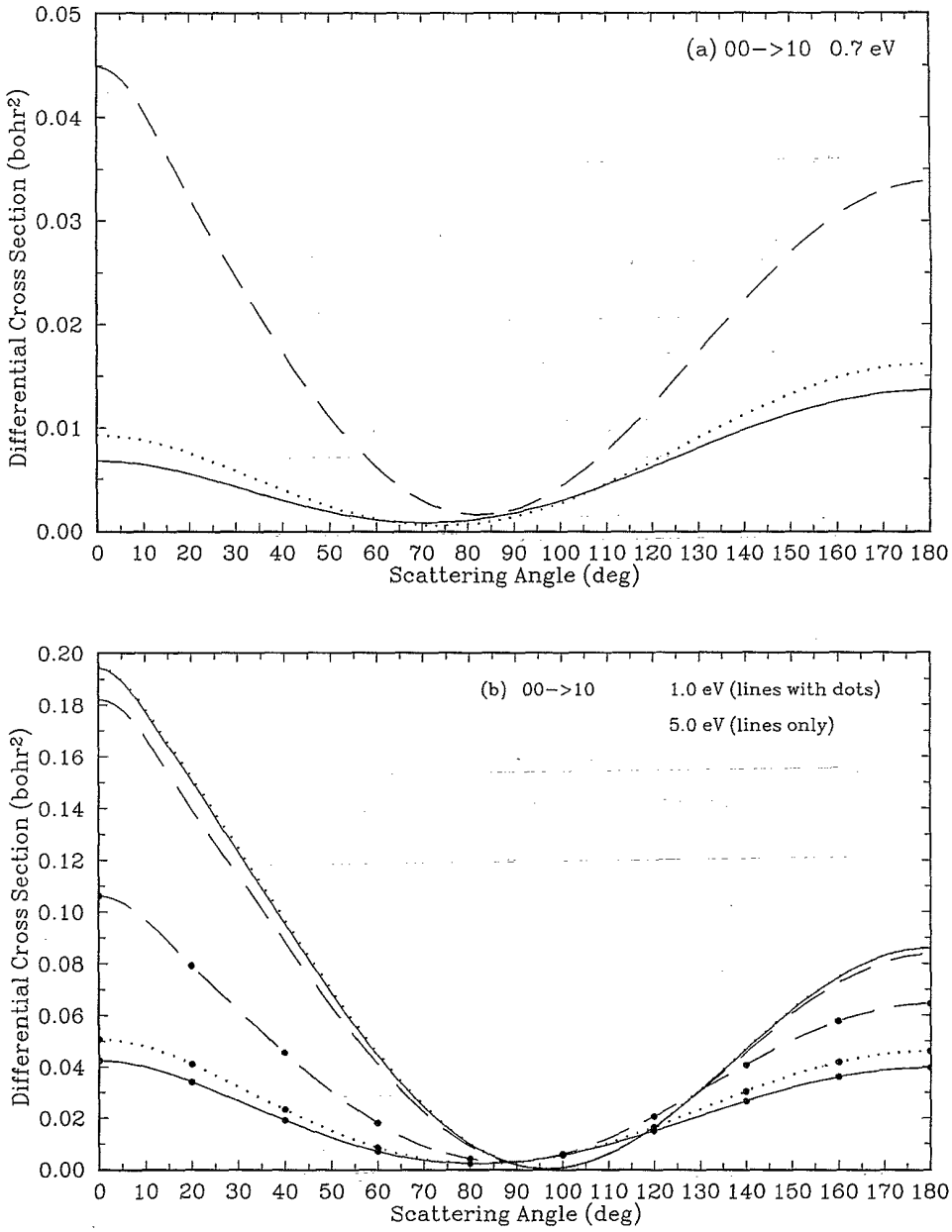

FIG. 6. Differential e-H_2 cross sections for pure vibrational excitation at (a) 0.7 eV and (b) 1.0 and 5.0 eV and for rovibrational excitation at (c) 0.7 eV and (d) 1.0 and 5.0 eV as calculated using three scattering theories: LFCC (solid curves), AN (long-dashed curves), and FONDA (dotted curves). All AN cross sections have been multiplied by k_{vj}/k_0.

quantifies the error caused by approximating the kernel by a local potential, neglecting the zero-point motion of the molecule, and assuming target-state degeneracy.

C. Vibrational excitation by a local potential

The most severe test of a scattering theory for inelastic electron-molecule collisions is vibrational excitation. We therefore conclude this appraisal of the FONDA method with cross section for pure vibrational and rovibrational excitation of H_2. The thresholds for these processes are[32,86] 0.516 eV for $0,0\rightarrow 1,0$ and 0.559 eV for $0,0\rightarrow 1,2$.

Figure 6 shows differential cross sections for these excitations at three energies as calculated using the LFCC, FONDA, and AN methods. The AN cross sections in these figures have been multiplied by k_{vj}/k_0 to force them to zero at threshold. The potential used in these calculations is a generalization of that of Sec. III B which allows for the variation in internuclear separation that accompanies the $v_0=0\rightarrow v=1$ excitation.[57,84]

For both $0,0\rightarrow 1,0$ and $0,0\rightarrow 1,2$, the greatest differences in the differential cross sections in this figure occur near threshold, at 0.7 eV (see also Fig. 1). Both the magnitude and shape of the AN cross section at this energy are quite different from the LFCC and FONDA results. To understand these differences and gain insight into the various approximations underlying this study—Born-Oppenheimer separability and target-state degeneracy—we shall "deconstruct" these cross sections with the aid of Eq. (56).

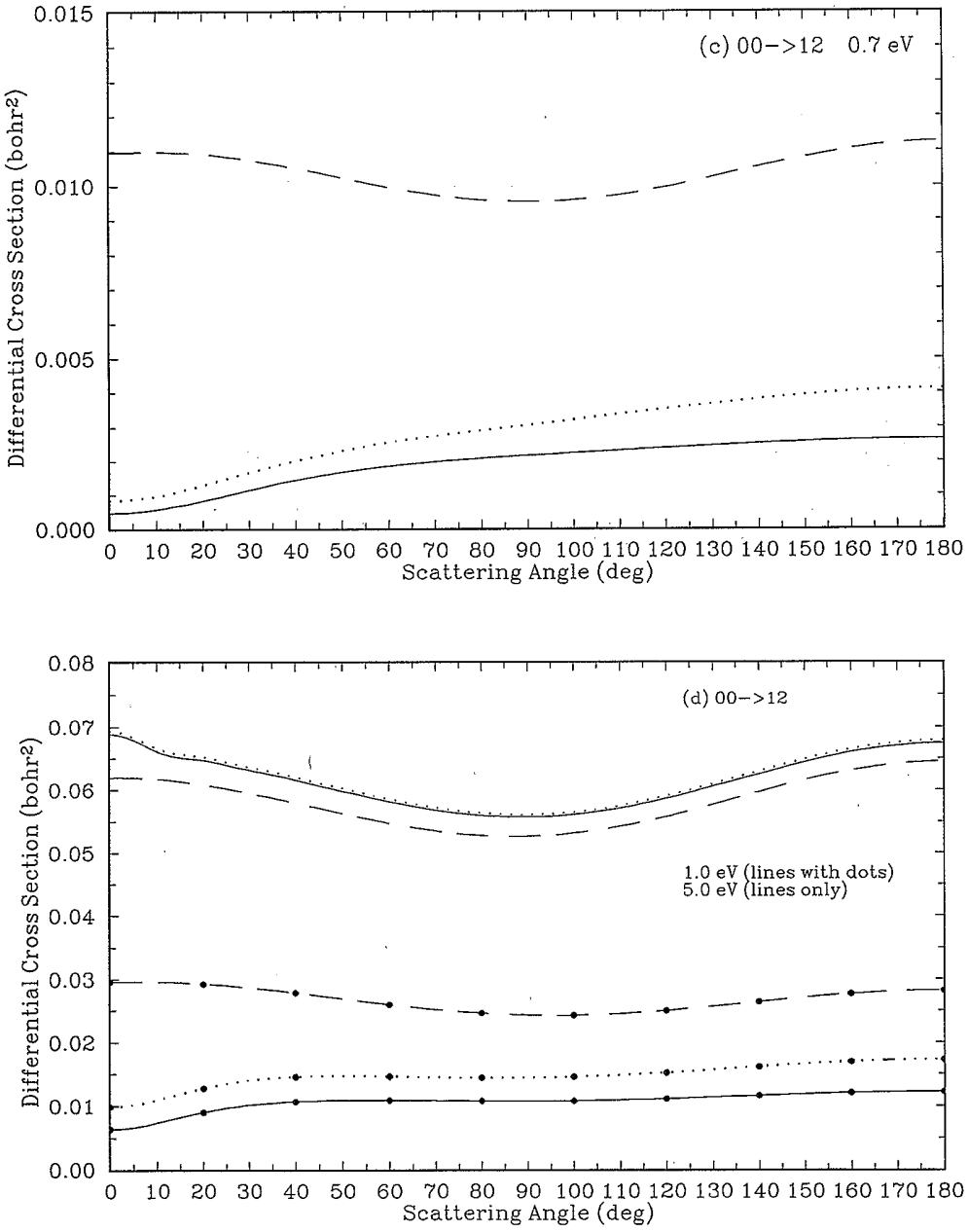

FIG. 6. (*Continued*).

TABLE IV. Percent contributions to e-H_2 rovibrational cross sections $\sigma_{v_0 j_0 \to vj}$ from various partial-waves in the entrance (l_0) and exit (l) channels.

	Pure vibrational excitation: 0,0→1,0			
	E=0.7 eV		E=1.0 eV	
$l_0 \to 1$	LFCC	AN	LFCC	AN
$p \to p$	68	86	85	90
$s \to s$	31	11	14	8
$f \to f$	0	0	0	1
	Rovibrational excitation: 0,0→1,2			
	E=0.7 eV		E=1.0 eV	
$l_0 \to l$	LFCC	AN	LFCC	AN
$p \to p$	90	99	98	99
$d \to s$	8	0	1	1
$f \to f$	2	1	0	0

The coefficient in this equation includes, in addition to a host of coupling coefficients, products of T-matrix elements whose interference significantly affects the shape of the differential cross section. Thus $A_{\lambda'}(v_0 j_0 \to vj)$ is a double sum over J_1, l_1, l_1' and J_2, l_2, l_2' of terms that include the product

$$T^{J_1 *}_{vjl_1, v_0 j_0 l_1'} T^{J_2 *}_{vjl_2, v_0 j_0 l_2'} . \tag{61}$$

In this coefficient there is a sum over λ, which identifies particular Legendre projections of the potential according to Eq. (33). This sum is controlled by three triangle rules that arise from Clebsch-Gordan coefficients: $\Delta(J_1 J_2 \lambda)$, $\Delta(l_1, l_2, \lambda)$, and $\Delta(l_1', l_2', \lambda)$.

At 0.7 eV, two terms in Eq. (56) dominate the pure vibrational cross section; for convenience we refer to them as the $p \to p$ and $s \to s$ terms. In Table IV we list their identifying quantum numbers and tabulate their percent contributions to $\sigma_{00 \to 10}$. Because of the aforementioned triangle rules, the $p \to p$ and $s \to s$ terms introduce different angular dependencies into the differential cross section for pure vibrational excitation.

The data in Table IV show that the errors in the AN approximation to this cross section arise in part from overrepresentation of the $p \to p$ contribution. According to Eq. (56), this overrepresentation gives excessive weight to Legendre polynomials with $\lambda > 0$, which, in turn, gives the AN result the unrealistically extreme angular dependence seen in Fig. 6(a). No such overrepresentation occurs in the FONDA or LFCC methods.

At higher energies, the breakdown in the AN approximation does not introduce so highly spurious an angular dependence. For example, at 1.0 eV, the percentage contributions in Table IV from the LFCC and AN calculations are comparable. At still higher energies, as Fig. 6 illustrates, the AN, LFCC, and FONDA methods produce essentially identical cross sections.

To conclude, we collect in Table V our LFCC, AN, and FONDA integrated vibrational excitation cross sections. This table quantifies the demonstrations in Fig. 1 that conservation of energy in the FONDA and LFCC methods is particularly important at energies from threshold to several tenths of an eV. In this energy range, AN cross sections, even when multiplied by k_{vj}/k_0, are in error by more than 100%, while the FONDA results agree with those from LFCC calculations to better than 15% for $v_0, j_0 = 0,0 \to v, j = 1,0$ and better than 45% for $v_0, j_0 \to v, j = 1,2$. With increasing energy, the FONDA cross sections become identical to LFCC (to within 1% numerical accuracy of these calculations), while the AN results remain in error to a few percent up to 10 eV.

V. CONCLUSIONS

The final equations of the FONDA method are (33)–(37) for a local potential and (51)–(53) for a potential that includes nonlocal terms. If only pure rotational excitation is of interest, then the vibrational matrix elements in these equations can be replaced with the potential at equilibrium (the rigid-rotor approximation), or more accurately, with the average of this potential over the ground vibrational state (the vibrational averaging approximation).[84]

However the potential is treated, the computational

TABLE V. e-H_2 rovibrational excitation cross sections (in units of a_0^2). Calculations based on a model exchange potential (see Sec. III).

	$v_0, j_0 = 0,0 \to v, j = 1,0$			$v_0, v_j = 0,0 \to v, j = 1,2$		
E (eV)	LFCC	FONDA	AN	LFCC	FONDA	AN
0.540	0.010	0.008	0.050	0.000	0.000	0.000
0.600	0.024	0.024	0.093	0.006	0.008	0.058
0.620	0.030	0.031	0.107	0.009	0.013	0.073
0.640	0.036	0.038	0.119	0.012	0.018	0.087
0.700	0.055	0.062	0.156	0.026	0.037	0.127
1.000	0.181	0.208	0.331	0.137	0.187	0.325
1.500	0.453	0.494	0.574	0.453	0.523	0.648
2.000	0.675	0.686	0.707	0.778	0.806	0.867
2.500	0.756	0.764	0.743	0.943	0.954	0.962
3.000	0.748	0.767	0.720	0.978	0.989	0.968
5.000	0.527	0.531	0.497	0.745	0.750	0.705
7.000	0.348	0.350	0.332	0.489	0.489	0.464
10.000	0.210	0.209	0.203	0.276	0.277	0.265

demands of the FONDA method are far less than those of a fully converged LFCC calculation. Even with the stringent numerical requirements of the present study, obtaining the FONDA results in Sec. IV took about one-third the CPU time required to solve the LFCC equations.

At the core of the FONDA theory are the BF FN radial functions $u^{\Lambda}_{l l_0}(r;R)$ that appear in the FONDA integrals. The solution of the BF FN equations for these functions has been thoroughly studied for a number of electron-molecule systems.[87] These studies provide a wealth of information about such practical matters as the requisite number of electron-molecule symmetries and partial waves, radial meshes for propagation of the scattering functions, the value of the radial coordinate at which the K matrix can be extracted, etc. So for many systems, implementation of the FONDA method, which as noted in Sec. II C 3 requires little additional code development, will also entail only a few numerical studies.

For e-H_2 scattering we have shown that because the FONDA approximation conserves energy, this method can produce rotational and vibrational excitation cross sections of much greater accuracy than those from the other approximate theories tested. There is, however, room for improvement in the accuracy of the FONDA vibrational excitation cross sections. The most likely source of error is the use of a Born-Oppenheimer separation outside the core of the molecule; in this region the interaction potential is less dominant than inside the core, and correct inclusion of the vibrational Hamiltonian may be important.[88] We are currently exploring an alternative formulation of the FONDA theory which treats the vibrational dynamics in this region exactly.

Separation of nuclear and projection variables outside the core is not imposed in theories such as the reformulation by Gao and Greene[89] of the energy-dependent vibrational frame transformation theory of Greene and Jungen;[90] this theory uses multichannel quantum-defect theory to allow for nonadiabatic behavior at large radial distances. Although essentially an on-shell theory, this formulation can accommodate additional nonadiabatic effects that are reflected in the dependence of the quantum-defect function on the body-frame energy. To date, Gao and Greene have studied the effects of this energy dependence in resonant and nonresonant scattering calculations using simplified models (s-wave scattering from a purely short-range potential) the electron-molecule system.

Having completed the formal development and evaluation of the FONDA method, we are turning to other electron-molecule systems, in particular to the important e-N_2 system.[91,92] In addition, we have begun formal and numerical extensions of the method to systems whose vibrational excitations exhibit strong structures very near threshold.[6]

ACKNOWLEDGMENTS

We are grateful to Wayne K. Trail and Dr. Bidhan C. Saha for their assistance with various aspects of the calculations reported here, to Dr. Thomas L. Gibson for his work on the extension of the FONDA theory to vibrational excitation, to Dr. Lee A. Collins and Dr. Greg Snitchler for advice concerning separable representations of exchange, and to Dr. Aaron Temkin and Dr. Chris Greene for useful conversations concerning breakdown of the adiabatic-nuclei theory. This research was supported by National Science Foundation Grant No. PHY-8505438 and utilized the CRAY 2 and XMP systems at the National Center for Supercomputing Applications at the University of Illinois at Urbana-Champaign.

*Present address: Department of Engineering, St. Mary's University, San Antonio, TX 78284-0440.

[1]A. V. Phelps in *Electron-Molecule Scattering*, edited by S. C. Brown (Wiley-Interscience, New York, 1979), Chap. 2; G. J. Schulz, in *Principles of Laser Plasmas*, edited by G. Bekite (Wiley, New York, 1976), Chap. 2.

[2]S. Trajmar, D. F. Register, and A. J. Chutjian, Phys. Rep. **97**, 220 (1983).

[3]M. A. Morrison, R. W. Crompton, B. C. Saha, and Z. Lj. Petrović, Aust. J. Phys. **40**, 239 (1987); R. W. Crompton and M. A. Morrison, in *Swarm Studies and Inelastic Electron-Molecule Scattering*, edited by L. C. Pitchford, V. McKoy, A. Chutjian, and S. Trajmar (Springer-Verlag, Berlin, 1986).

[4]N. F. Lane, Rev. Mod. Phys. **52**, 29 (1980).

[5]L. A. Collins and D. W. Norcross, Adv. At. Mol. Phys. **18**, 341 (1983).

[6]M. A. Morrison, Adv. At. Mol. Phys. **24**, 51 (1988).

[7]P. G. Burke, Adv. At. Mol. Phys. **15**, 471 (1979).

[8]A. M. Arthurs and A. Dalgarno, Proc. R. Soc. London Ser. A **256**, 540 (1960).

[9]N. F. Lane and S. Geltman, Phys. Rev. **160**, 53 (1967).

[10]R. J. W. Henry and N. F. Lane, Phys. Rev. **183**, 221 (1969).

[11]D. M. Chase, Phys. Rev. A **104**, 838 (1956).

[12]A. Temkin and K. V. Vasavada, Phys. Rev. **160**, 190 (1967); A. Temkin, K. V. Vasavada, E. S. Chang, and A. Silver, **186**, 58 (1969).

[13]S. Hara, J. Phys. Soc. Jpn. **27**, 1592 (1969).

[14]A. Temkin and F. H. M. Faisal, Phys. Rev. A **3**, 520 (1971); F. H. M. Faisal and A. Temkin, Phys. Rev. Lett. **28**, 203 (1972).

[15]A. Temkin and E. C. Sullivan, Phys. Rev. Lett. **33**, 1057 (1974).

[16]E. S. Chang and A. Temkin, Phys. Rev. A **23**, 399 (1969).

[17]M. Shugard and A. U. Hazi, Phys. Rev. A **12**, 1895 (1975).

[18]See, for example, T. N. Rescigno, A. E. Orel, and V. McKoy, Phys Rev. A **26**, 690 (1982); A. Jain and D. G. Thompson, J. Phys. B **16**, 2593 (1983).

[19]A. N. Feldt and M. A. Morrison, J. Phys. B **15**, 301 (1982).

[20]M. A. Morrison, A. N. Feldt, and D. Austin, Phys. Rev. A **29**, 2518 (1984).

[21]M. A. Morrison, A. N. Feldt, and B. C. Saha, Phys. Rev. A **30**, 2811 (1984).

[22]A number of investigators have recently explored alternative approaches to the problem of low-energy inelastic scattering. See, for example, E. Ficocelli Varracchio, and U. T. Lamanna, J. Phys. B **19**, 3145 (1987); W. Domcke and C. Mündel, J. Phys. B **18**, 4491 (1985), and H. Gao and C. Greene, J. Chem.

Phys. **91**, 3988 (1989).
[23]M. A. Morrison, J. Phys. B **19**, L707 (1986).
[24]Department of Applied Mathematics and Theoretical Physics, The Queen's University of Belfast, Belfast BT7 1NN, Northern Ireland.
[25]M. A. Morrison, Comput. Phys. Commun. **21**, 63 (1980); L. A. Collins, D. W. Norcross, and G. B. Schmid, *ibid.* **21**, 79 (1980); W. E. Weitzel, III, T. L. Gibson, and M. A. Morrison, *ibid.* **30**, 161 (1983).
[26]G. Raseev, Comput. Phys. Commun. **20**, 275 (1980); A. L. Sinfailam, *ibid.* **1**, 445 (1970).
[27]M. A. Brandt, D. G. Truhlar, and R. L. Smith, Comput. Phys. Commun. **5**, 456 (1973); K. Onda, D. G. Truhlar, and M. A. Brandt, *ibid.* **21**, 97 (1980); S. A. Salvini, *ibid.* **27**, 25 (1982); S. A. Salvini and D. G. Thompson, *ibid.* **22**, 49 (1981); R. J. W. Henry, *ibid.* **10**, 375 (1975).
[28]M. A. Abdolsalami and M. A. Morrison, Phys. Rev. A **36**, 5474 (1987).
[29]In this section we use the notation of Sec. II of Ref. 6; this reference contains a summary of canonical LFCC, AN, and BFVCC theory in this notation.
[30]For a tutorial-style overview of the main concepts of electron-molecule scattering, see M. A. Morrison, Aust. J. Phys. **36**, 239 (1983).
[31]K. P. Huber and G. Herzberg, *Molecular Spectra and Molecular Structure IV. Constants of Diatomic Molecules* (Van Nostrand, New York, 1979).
[32]A. A. Radzig and B. Smirnov, *Reference Data on Atoms, Molecules, and Ions* (Springer-Verlag, New York, 1986).
[33]J. R. Taylor, *Scattering Theory* (Wiley, New York, 1972).
[34]M. Born and J. R. Oppenheimer, Ann. Phys. (Leipzig) **84**, 457 (1927).
[35]M. A. Morrison, T. L. Estle, and N. F. Lane, *Quantum States of Atoms, Molecules, and Solids* (Prentice-Hall, Engelwood Cliffs, NJ, 1977), Chap. 12.
[36]W. Kolos, Adv. Quant. Chem. **5**, 99 (1971).
[37]C. J. Joachain, *Quantum Collision Theory* (North-Holland, New York, 1975), Chap. 16.
[38]If one neglects this dependence (by, say, evaluating $\bar{f}_0$ at the equilibrium geometry), then Eq. (12a) becomes equivalent to the coupled equations of two-state close-coupling theory with the final-state potential $V_{vv}(r)$ set equal to zero.
[39]R. J. W. Henry, Phys. Rev. A **2**, 1349 (1970).
[40]W. H. Flygare, *Molecular Structure and Dynamics* (Prentice-Hall, Englewood Cliffs, NJ, 1978).
[41]See M. E. Rose, *Elementary Theory of Angular Momentum* (Wiley, New York, 1957).
[42]See Sec. II B of Ref. 6.
[43]See Sec. IV of the review by D. E. Golden, N. F. Lane, A. Temkin, and E. Gerjuoy, Rev. Mod. Phys. **43**, 642 (1971).
[44]M. A. Morrison and G. A. Parker, Aust. J. Phys. **40**, 465 (1987).
[45]E. S. Chang and U. Fano, Phys. Rev. A **6**, 173 (1972).
[46]See Sec. II D of Ref. 6 and references therein.
[47]In the rigid-rotor approximation, with molecular vibrations completely ignored, the integral over R disappears and the FONDA K matrix is defined at the equilibrium separation only (see Ref. 23). For a very simple alternative to the rigid-rotor approximation which introduces the zero-point vibrational motion and markedly improves the resulting elastic and rotational excitation cross sections, see Ref. 84.
[48]D. W. Norcross and N. T. Padial, Phys. Rev. A **25**, 226 (1982).
[49]S. Hara, J. Phys. Soc. Jpn. **22**, 710 (1967).
[50]M. A. Morrison and L. A. Collins, Phys. Rev. A **17**, 918 (1978); **23**, 127 (1981).
[51]J. K. O'Connell and N. F. Lane, Phys. Rev. A **27**, 1893 (1983); N. T. Padial and D. W. Norcross, *ibid.* **29**, 1742 (1984); **29**, 1590 (1984); N. T. Padial, *ibid.* **32**, 1379 (1985); A. Jain and D. W. Norcross, *ibid.* **32**, 134 (1985); **84**, 739 (1986); P. K. Bhattacharyya, D. K. Syamal, and B. C. Saha, *ibid.* **32**, 854 (1985).
[52]N. T. Padial, D. W. Norcross, and L. A. Collins, J. Phys. B **14**, 2901 (1981).
[53]B. I. Schneider and L. A. Collins, Phys. Rev. A **24**, 1264 (1981); L. A. Collins and B. I. Schneider, *ibid.* **34**, 1564 (1986); T. N. Rescigno and A. E. Orel, *ibid.* **23**, 1234 (1981); **24**, 1267 (1981); **25**, 2402 (1982); H.-D. Meyer, *ibid.* **34**, 1797 (1986); H. Kutz and H.-D. Meyer, J. Phys. B **23**, 829 (1990); L. Malegat, M. Le Dourneuf, and Vo Ky Lan, *ibid.* **20**, 4143 (1987).
[54]G. Snitchler, D. Norcross, A. Jain, and S. Alston, Phys. Rev. A **42**, 671 (1990).
[55]W. H. Press, B. P. Flannery, S. A. Teukolsky, and W. T. Vetterling, *Numerical Recipes: The Art of Scientific Computing* (Cambridge University Press, New York, 1986).
[56]A. Erdelyi, W. Magnus, F. Oberhettinger, and F. T. Tricomi, *Tables Of Integrated Transforms* (McGraw-Hill, New York, 1954), pp. 121 and 187; A. Fliflet, D. Levin, M. Ma, and V. McKoy, Phys. Rev. A **17**, 160 (1978); M. Berman and U. Kaldor, J. Phys. B **14**, 3993 (1981).
[57]M. A. Morrison and B. C. Saha, Phys. Rev. A **34**, 2786 (1986).
[58]J. W. Moskowitz and L. C. Snyder, in *Methods of Electronic Structure Theory,* edited by H. F. Schaeffer, III (Plenum, New York, 1977), p. 387.
[59]S. Huzinaga, J. Chem. Phys. **43**, 1293 (1965).
[60]T. H. Dunning, J. Chem. Phys. **53**, 2823 (1970); **55**, 3958 (1971).
[61]W. Kolos and C. C. Roothaan, Rev. Mod. Phys. **21**, 205 (1960); L. Laaksonen, P. Pyykko, and D. Sundholm, Int. J. Quantum. Chem. **23**, 319 (1983).
[62]K. B. MacAdam and N. F. Ramsey, Phys. Rev. A **6**, 898 (1972).
[63]T. L. Gibson and M. A. Morrison, J. Phys. B **14**, 727 (1981).
[64]T. L. Gibson and M. A. Morrison, Phys. Rev. A **29**, 2497 (1984); M. A. Morrison, B. C. Saha, and T. L. Gibson, *ibid.* **36**, 3682 (1987).
[65]A. Temkin, Phys. Rev. **107**, 1004 (1957).
[66]W. Kolos and L. Wolniewicz, J. Chem. Phys. **46**, 1426 (1976).
[67]A. C. Newell and R. C. Baird, J. Appl. Phys. **36**, 3751 (1965).
[68]M. A. Morrison, G. D. Danby, W. K. Trail, and B. K. Elza (unpublished).
[69]D. R. Hartree, *The Calculation of Atomic Structures* (Wiley, New York, 1957).
[70]Detailed expressions for the coefficient A_λ appear in Ref. 8. See also Ref. 4.
[71]This procedure is described in Sec. IV B 2 of Ref. 20.
[72]For a description of this procedure, see Sec. III C of Ref. 84.
[73]B. D. Buckley, P. G. Burke, and C. J. Noble, in *Electron-Molecule Collisions,* edited by I. Shimamura and K. Takayanagi (Plenum, New York, 1984), p. 495.
[74]L. A. Collins, W. D. Robb, and M. A. Morrison, J. Phys. B **11**, L777 (1978); Phys. Rev. A **21**, 488 (1980).
[75]B. I. Schneider and L. A. Collins, J. Phys. B **14**, L101 (1981); L. A. Collins and B. I. Schneider, Phys. Rev. A **27**, 2387 (1981); **27**, 101 (1983).
[76]J. N. Bardsley and R. K. Nesbet, Phys. Rev. A **8**, 203 (1973).
[77]See Sec. IV A of Ref. 6.
[78]K. Jung, K-M. Scheuerlein, W. Sohn, K-H. Kochem, and H. Ehrhardt, J. Phys. B **80**, L327 (1987).
[79]R. K. Nesbet, Phys. Rev. A **19**, 551 (1979).

[80]C. Mündel, M. Berman, and W. Domcke, Phys. Rev. A **32**, 181 (1985).
[81]A. N. Feldt and M. A. Morrison, Phys. Rev. A **29**, 401 (1984).
[82]E. Gerjuoy and S. Stein, Phys. Rev. **97**, 1671 (1955).
[83]A. Dalgarno and R. J. Moffett, Proc. Natl. Acad. Sci. India **33**, 511 (1963).
[84]W. K. Trail, M. A. Morrison, W. A. Isaacs, and B. C. Saha, Phys. Rev. A **41**, 4868 (1990).
[85]J. P. England, M. T. Elford, and R. W. Crompton, Aust. J. Phys. **41**, 573 (1988).
[86]The molecular constants of the ground electronic state of H_2 used in this work are $B_0=60.855$ cm^{-1}, $\alpha_e=3.062$ cm^{-1}, $\omega_e=4401.320$ cm^{-1}, and $\omega_e x_e=121.333$ cm^{-1}.
[87]Valuable technical discussions of these matters appear in Ref. 73 and in articles in *Electron Molecule and Photon-Molecule Collisions,* edited by T. N. Rescigno, V. McKoy, and B. I. Schneider (Plenum, New York, 1979), and in *Electron-Molecule Interactions and Their Applications, Volume 1,* edited by L. G. Christophorou (Academic, New York, 1984). An extensive discussion of results up to 1979 can be found in Ref. 4; this data is updated by Ref. 6 and F. A. Gianturco and A. Jain, Phys. Rep. **143**, 347 (1986).
[88]U. Fano, Comments At. Mol. Phys. **1**, 140 (1970).
[89]H. Gao and C. H. Greene, J. Chem. Phys. **91**, 3988 (1989).
[90]C. H. Greene and Ch. Jungen, Adv. At. Mol. Phys. **21**, 51 (1985).
[91]B. I. Schneider and L. A. Collins, Comput. Phys. Commun. **53**, 381 (1989).
[92]B. I. Schneider and L. A. Collins, Comput. Phys. Rep. **10**, 51 (1989).